

T H E U N I V E R S I T Y O F M I C H I G A N

COLLEGE OF ENGINEERING
Department of Electrical Engineering
Space Physics Research Laboratory

Sounding Rocket Flight Report

NASA 18.104 AND NASA 18.105
THERMOSPHERE PROBE EXPERIMENTS

Prepared on behalf of the project by

H. J. Grassl

ORA Project 027700

under contract with:

NATIONAL AERONAUTICS AND SPACE ADMINISTRATION
GODDARD SPACE FLIGHT CENTER
CONTRACT NO. NAS 5-21038
GREENBELT, MARYLAND

administered through:

OFFICE OF RESEARCH ADMINISTRATION ANN ARBOR

February 1971

TABLE OF CONTENTS

	Page
LIST OF ILLUSTRATIONS	iv
1. INTRODUCTION	1
2. GENERAL FLIGHT INFORMATION	2
3. LAUNCH VEHICLE	4
4. NOSE CONE	7
5. THE THERMOSPHERE PROBE (TP)	
5.1. Omegatron	10
5.2. Electron Temperature and Density Probe	17
5.3. Support Measurements and Instrumentation	
5.3.1. Aspect determination system	20
5.3.2. Telemetry	23
5.3.3. Housekeeping monitors	24
6. ANALYSIS OF DATA	25
6.1. Trajectory and Aspect	25
6.2. Ambient N ₂ Density	28
6.3. Temperature	38
6.4. Geophysical Indices	38
7. REFERENCES	43

LIST OF ILLUSTRATIONS

Table	Page
I. Table of Events	3
II. Omegatron Data	12
III. N ₂ Ambient Density Data	28

Figure	Page
1. Nike-Tomahawk with thermosphere probe payload.	5
2. Nike-Tomahawk dimensions.	6
3. Thermosphere probe instrumentation design.	8
4. Assembly drawing, 8-in. nose cone.	9
5. Thermosphere probe system block diagram.	11
6. Omegatron II.	14
7. Final calibration of the NASA 18.104 omegatron.	15
8. Final calibration of the NASA 18.105 omegatron.	16
9. Electron temperature and density probe.	18
10. ETDP system timing and output format.	19
11. NASA 18.104 minimum angle of attack vs. altitude.	21
12. NASA 18.105 minimum angle of attack vs. altitude.	22
13. NASA 18.104 sequence of events.	26
14. NASA 18.105 sequence of events.	27
15. NASA 18.104 omegatron current vs. flight time.	30
16. NASA 18.105 omegatron current vs. flight time.	31

LIST OF ILLUSTRATIONS (Concluded)

Figure		Page
17.	$K(S_o, \alpha)$ vs. altitude for NASA 18.104.	32
18.	$K(S_o, \alpha)$ vs. altitude for NASA 18.105.	33
19.	NASA 18.104 ambient N_2 density vs. altitude.	34
20.	NASA 18.105 ambient N_2 density vs. altitude.	35
21.	NASA 18.104 neutral particle temperature vs. altitude.	39
22.	NASA 18.105 neutral particle temperature vs. altitude.	40
23.	Solar flux at 10.7 cm wavelength.	41
24.	Three-hour geomagnetic activity index (a_p).	42

1. INTRODUCTION

The results of NASA 18.104 and NASA 18.105, identical Nike-Tomahawk sounding rockets launched during the solar eclipse of March 1970, are presented and discussed in this report. The payload for each flight, a Thermosphere Probe (TP), described by Spencer, Brace, Carignan, Tausch, and Niemann (1965), was jointly developed by the Space Physics Research Laboratory (SPRL) of The University of Michigan and the Goddard Space Flight Center (GSFC), Laboratory for Planetary Atmospheres. The TP is an ejectable instrument package designed for the purpose of studying the variability of the earth's atmospheric parameters in the altitude region between 120 and 350 km. Each payload included a "second generation" omegatron mass analyzer, an ion spectrometer, an electron temperature probe (Spencer, and Carignan, 1962), and a solar position sensor. This complement of instruments permitted the determination of the molecular nitrogen density and temperature and the charged particle density and temperature in the altitude range of approximately 150 to 290 km over Wallops Island, Virginia, during 40% (NASA 18.104) and 80% (NASA 18.105) solar obscuration.

A general description of the payload kinematics, orientation analysis, and the technique for the reduction and analysis of the data is given by Tausch, Carignan, Niemann, and Nagy (1965) and Carter (1968). The $f(s)$ curve fitting technique for reduction of the omegatron data is not described here but will be presented in a future report, currently in preparation. The orientation analysis and the reduction of the nitrogen data were performed at SPRL, and the results are included in this report. The ion spectrometer data and the electron temperature probe data were reduced at GSFC, and are not discussed here.

2. GENERAL FLIGHT INFORMATION

The general flight information for NASA 18.104 and NASA 18.105 is listed below. Table I gives the flight times and altitudes of significant events which occurred during the flights. Some of these were estimated and are so marked. The others were obtained from the telemetry records and radar trajectory information.

Flight:	NASA 18.104	NASA 18.105
Launch Date:	07 March 1970	07 March 1970
Launch Time:	18:00:00.079 GMT	18:27:00.073 GMT
Location:	Wallops Island, Virginia	Wallops Island, Virginia
	Latitude: 37°50'14.915"N	Latitude: 37°50'14.915"N
	Longitude: 75°29'01.693"W	Longitude: 75°29'01.693"W

Apogee Parameters:

Altitude:	289.32 km	290.21 km
Horizontal Velocity:	277.2 m/sec	343.8 m/sec
Flight Time:	265.5 sec	266.0 sec

TP Motion:

Tumble Period:	11.158 sec	2.451 sec
Roll Rate:	47.14 deg/sec	~147 deg/sec

TABLE I

TABLE OF EVENTS

Event	NASA 18.104		NASA 18.105	
	Flight Time (sec)	Altitude (km)	Flight Time (sec)	Altitude (km)
Lift-off	0	0	0	0
1st Stage Burnout	3.6	1.4	3.9	1.6
2nd Stage Ignition	12.0	6.6	12.1	6.7
2nd Stage Burnout	21.8	20.2	21.5	19.5
Despin	----	----	43.6 (est.)	66.9 (est.)
TP Ejection	45.8	71.3	45.6	70.9
Omegatron Breakoff	78.3	131.5	78.7	132.3
Omegatron Filament On	80.8	135.7	79.9	134.3
Peak Altitude	265.5	289.32	266.0	290.21
L. O. S.	502.0	----	498.0	----

3. LAUNCH VEHICLE

The launch vehicles for NASA 18.104 and NASA 18.105 were two-stage, solid propellant Nike-Tomahawk combinations. The first stage of each vehicle, a Hercules M5E1 Nike motor, had an average thrust of 49,000 lb and burned for approximately 3.6 sec. The Nike booster, plus adapter, was 145.2 in. long and 16.5 in. in diameter. Its weight unburned was approximately 1325 lb. The sustainer stage, Thiokol's TE416 Tomahawk motor, provided an average thrust of 11,000 lb and burned for about 9 sec. The Tomahawk, 141.4 in. long and 9 in. in diameter, weighed 530 lb unburned. Each TP payload, which was 90.5 in. long and weighed 175 lb including despin and adapter modules, made the total vehicle 377.1 in. long with a gross lift-off weight of 2030 lb. The vehicle is illustrated in Figures 1 and 2.

Both launch vehicles performed flawlessly. NASA 18.104 reached a summit altitude of 289.32 km at 265.5 sec of flight time, and NASA 18.105 reached a summit altitude of 290.21 at 266.0 sec of flight time.

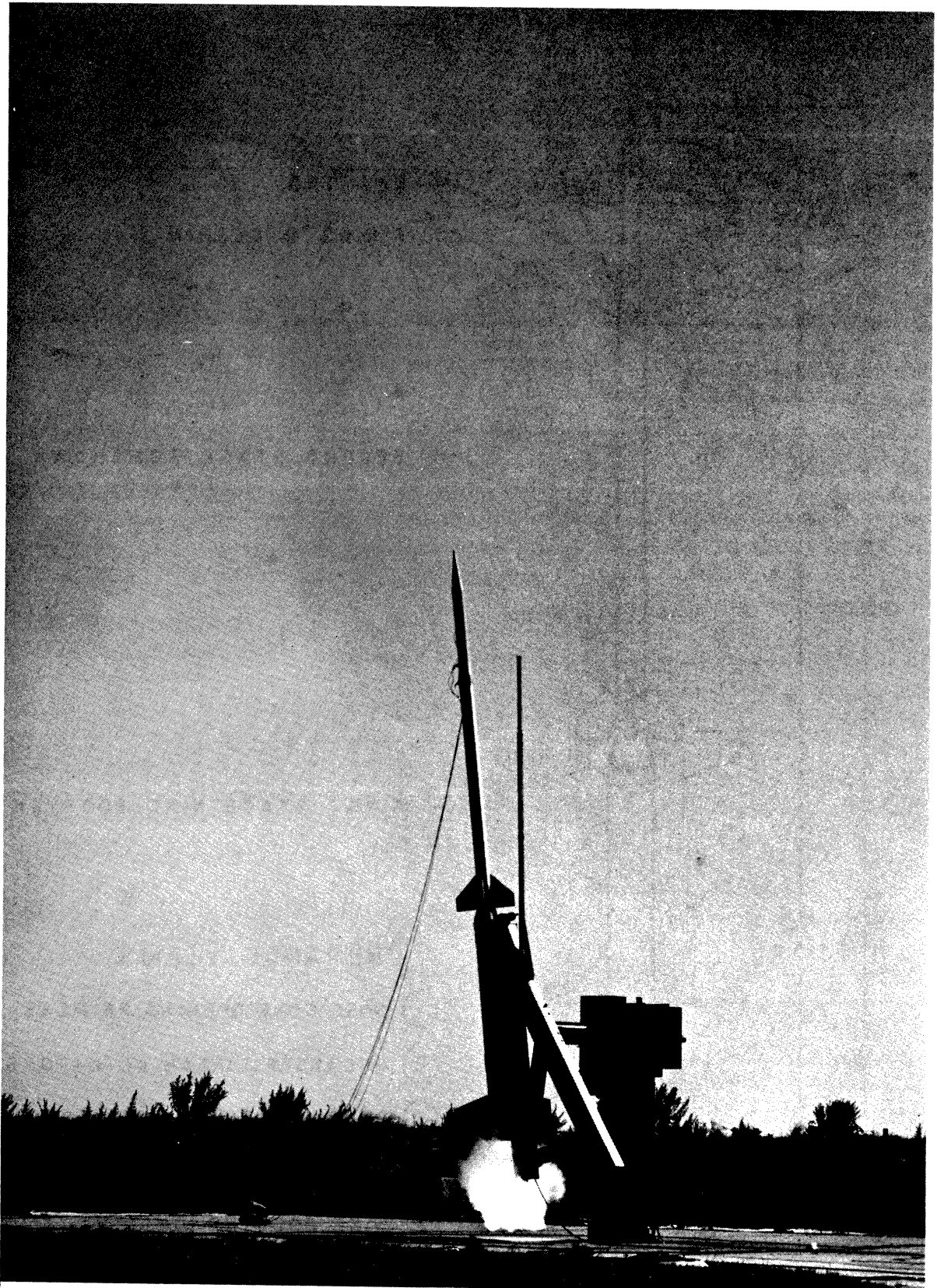


Figure 1. Nike-Tomahawk with thermosphere probe payload.

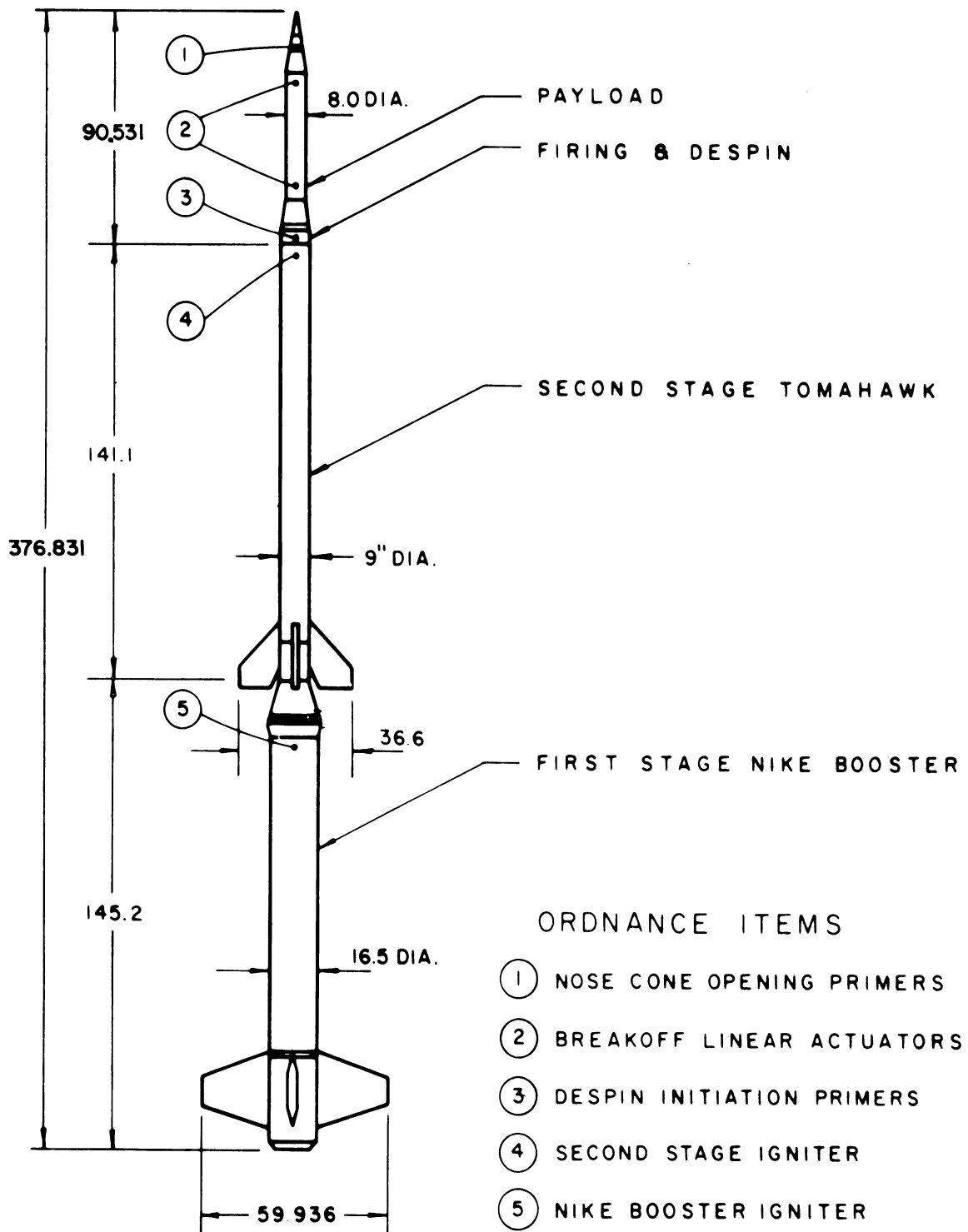


Figure 2. Nike-Tomahawk dimensions.

4. NOSE CONE

A diagram of the payload for both NASA 18.104 and NASA 18.105 including the nose cone, the despin mechanism, and the adapter section is shown in Figure 3. An assembly drawing of the 8-in. nose cone is given in Figure 4.

The despin mechanism on NASA 18.104 apparently did not work. Ejection began at 71 km (46 sec after launch), and the resulting tumble period was 11.158 sec. The omegatron breakoff device was removed at 132 km (78 sec after launch), and the omegatron filament was turned on approximately 2 sec later.

The NASA 18.105 payload was despun at 67 km (44 sec after launch), and the ejection began at 71 km (46 sec after launch). The resulting tumble period of the payload was 2.451 sec. The omegatron breakoff device was removed at 132 km (79 sec after launch), and the omegatron filament was turned on approximately 2 sec later.

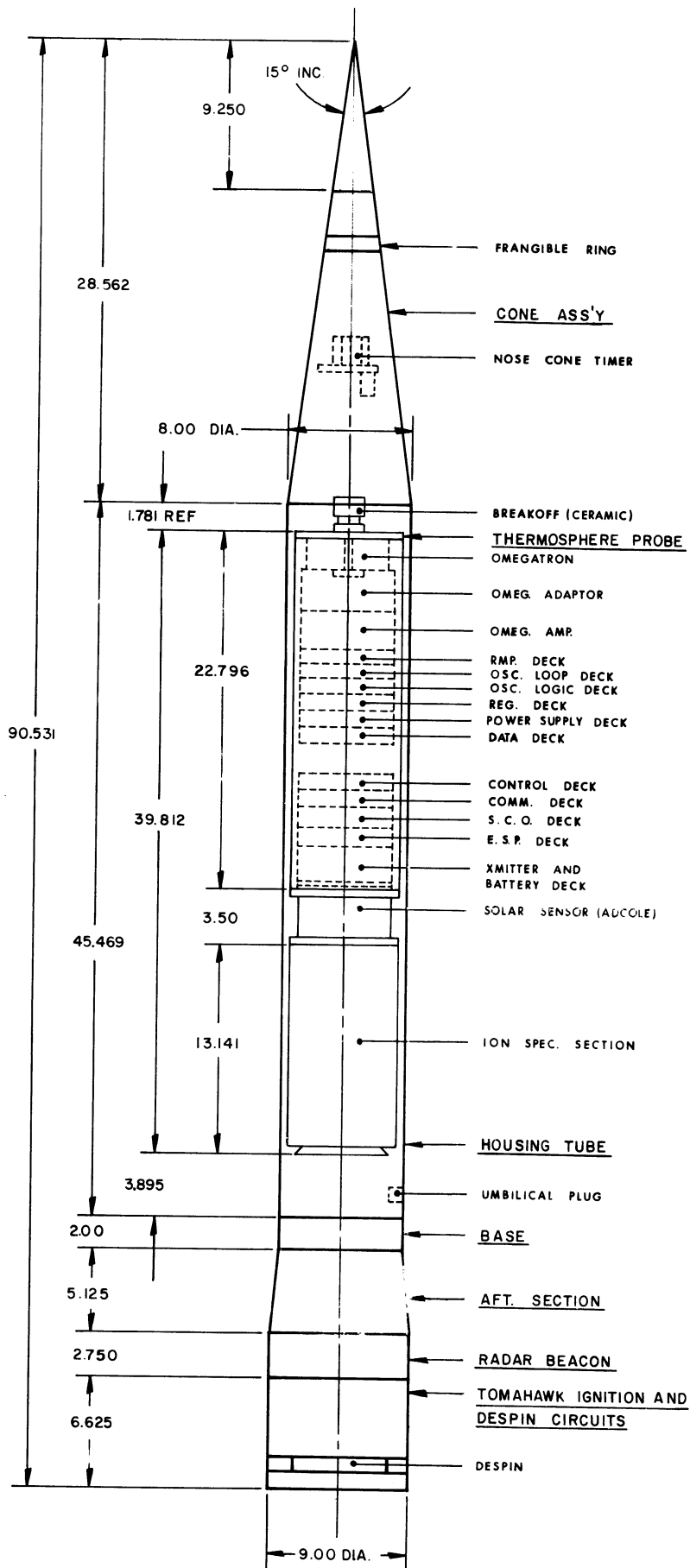


Figure 3. Thermosphere probe instrumentation design.

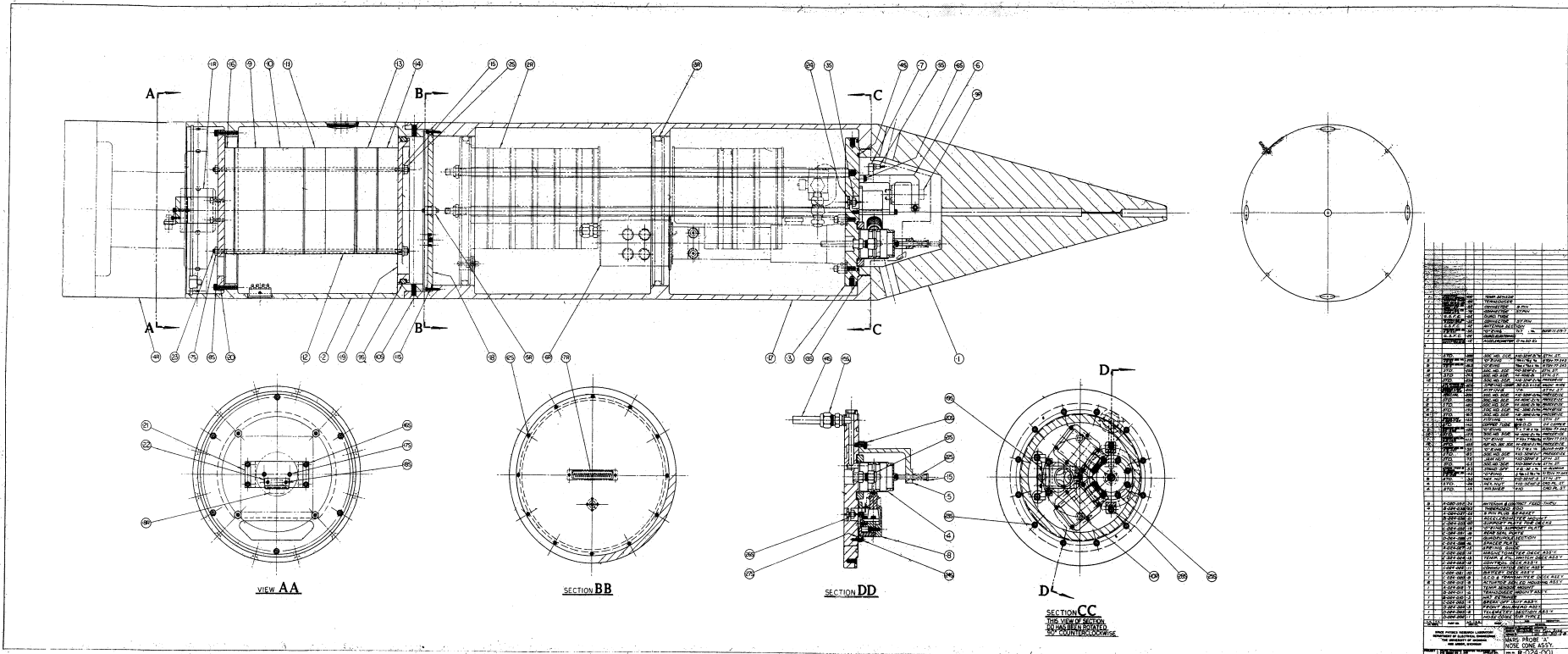


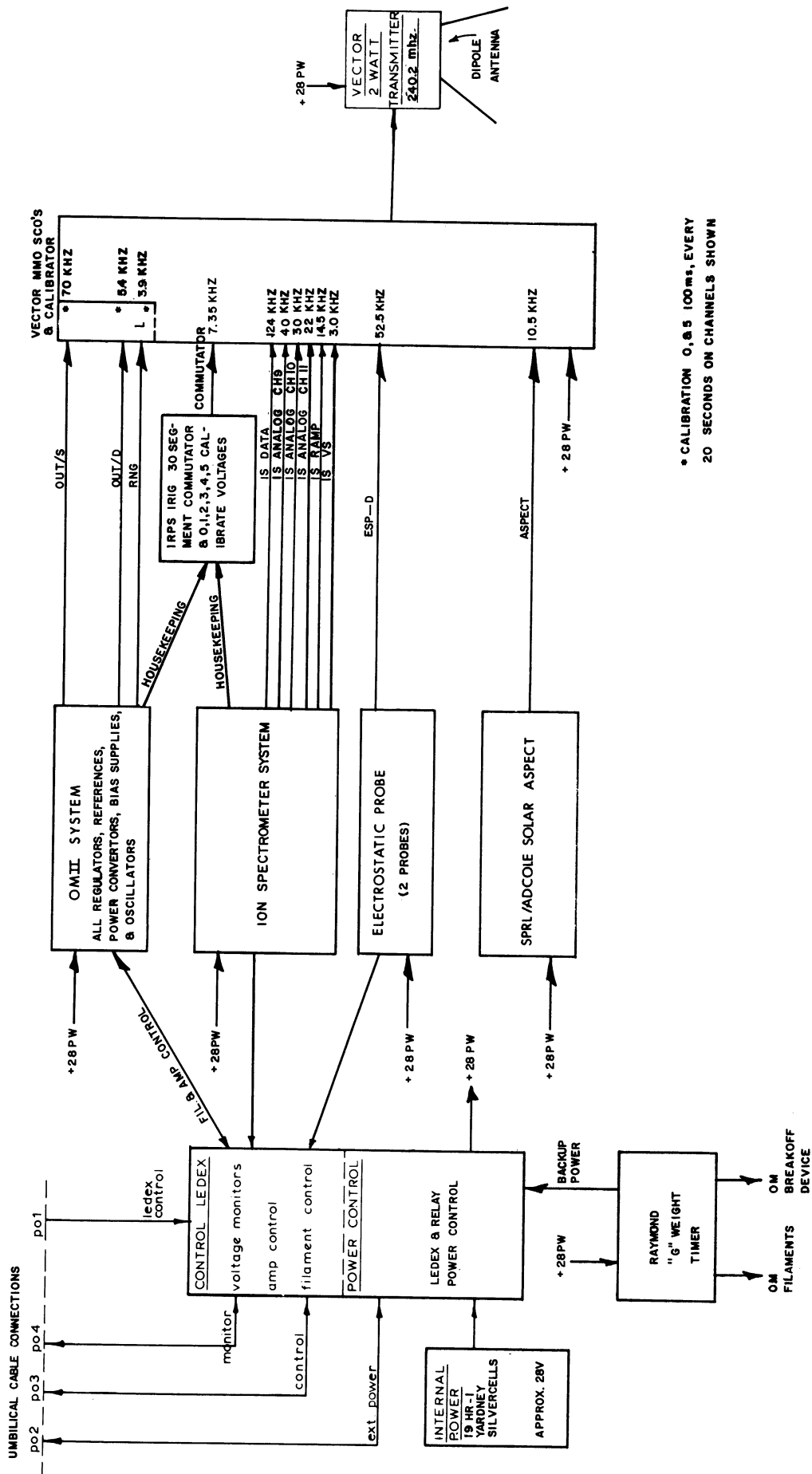
Figure 4. Payload assembly.

5. THERMOSPHERE PROBE

The TPs used for the NASA 18.104 and NASA 18.105 payloads were cylinders 39.8 in. long and 7.25 in. in diameter and weighed 75 lb. each. The major instrumentation of each payload included an Omegatron II mass analyzer, an ion spectrometer, and an electron temperature probe. Supporting instrumentation included a solar aspect sensor for use in determining the attitude of the TP. The diagram in Figure 3 shows the location of instrumentation and supporting electronics in the nose cone and Figure 5 is the system block diagram for both probes.

5.1. OMEGATRON

Table II lists the sensitivity of the omegatrons and the characteristics of the linear electrometer amplifier current detector used to monitor the omegatron output currents. The omegatron envelope and breakoff configuration are shown in Figure 6. The calibrations of the NASA 18.104 and NASA 18.105 omegatrons, performed at SPRL during January 1970, are shown in Figures 7 and 8.



* CALIBRATION 0.65 100ms, EVERY 20 SECONDS ON CHANNELS SHOWN

Figure 5. Thermosphere probe system block diagram.

TABLE II

OMEGATRON DATA

(NASA 18.104)

CalibrationNormalized N₂ Sensitivity: 1.64×10^{-5} A/torrElectrometer Amplifier

OUT/S

<u>Range</u>	<u>Range</u>		<u>Gain</u>	<u>Bias</u>
	<u>Indicator</u>	<u>Resistor</u>		
1-1	0.54 V	1.000×10^{12}	-1.98	+ 1.42 V
1-2	0.83 V	1.000×10^{12}	-1.98	- 2.56 V
1-3	1.13 V	1.000×10^{12}	-0.99	- 3.03 V
1-4	1.43 V	1.000×10^{12}	-0.99	- 7.00 V
1-5	1.73 V	1.000×10^{12}	-0.99	-10.97 V
1-6	2.03 V	1.000×10^{12}	-0.99	-14.94 V
1-7	2.33 V	1.000×10^{12}	-0.99	-18.89 V
2-1	2.81 V	6.664×10^{10}	-1.98	+ 1.42 V
2-2	3.13 V	6.664×10^{10}	-1.98	- 2.56 V
2-3	3.45 V	6.664×10^{10}	-0.99	- 3.03 V
2-4	3.76 V	6.664×10^{10}	-0.99	- 7.00 V
2-5	4.07 V	6.664×10^{10}	-0.99	-10.97 V
2-6	4.39 V	6.664×10^{10}	-0.99	-14.94 V
2-7	4.70 V	6.664×10^{10}	-0.99	-18.89 V

OUT/D

<u>Range</u>	<u>Range</u>		<u>Gain</u>	<u>Bias</u>
	<u>Indicator</u>	<u>Resistor</u>		
1	—	1.000×10^{12}	-0.2486	- 0.0059 V
2	—	6.664×10^{10}	-0.2486	- 0.0059 V

TABLE II (Concluded)

(NASA 18.105)

Calibration

Normalized N₂ Sensitivity: 1.68 x 10⁻⁵ A/torr

Electrometer Amplifier

OUT/S

<u>Range</u>	<u>Range</u>		<u>Gain</u>	<u>Bias</u>
	<u>Indicator</u>	<u>Resistor</u>		
1-1	0.55 V	1.000 x 10 ¹²	-1.99	+ 1.39 V
1-2	0.85 V	1.000 x 10 ¹²	-1.99	- 2.61 V
1-3	1.14 V	1.000 x 10 ¹²	-0.99	- 3.07 V
1-4	1.44 V	1.000 x 10 ¹²	-0.99	- 7.05 V
1-5	1.74 V	1.000 x 10 ¹²	-0.99	-11.04 V
1-6	2.04 V	1.000 x 10 ¹²	-0.99	-15.03 V
1-7	2.34 V	1.000 x 10 ¹²	-0.99	-18.99 V
2-1	2.82 V	6.664 x 10 ¹⁰	-1.99	+ 1.39 V
2-2	3.14 V	6.664 x 10 ¹⁰	-1.99	- 2.61 V
2-3	3.46 V	6.664 x 10 ¹⁰	-0.99	- 3.07 V
2-4	3.77 V	6.664 x 10 ¹⁰	-0.99	- 7.05 V
2-5	4.08 V	6.664 x 10 ¹⁰	-0.99	-11.04 V
2-6	4.40 V	6.664 x 10 ¹⁰	-0.99	-15.03 V
2-7	4.71 V	6.664 x 10 ¹⁰	-0.99	-18.99 V

OUT/D

<u>Range</u>	<u>Range</u>		<u>Gain</u>	<u>Bias</u>
	<u>Indicator</u>	<u>Resistor</u>		
1	—	1.000 x 10 ¹²	-0.2487	- 0.0075 V
2	—	6.664 x 10 ¹⁰	-0.2487	- 0.0075 V

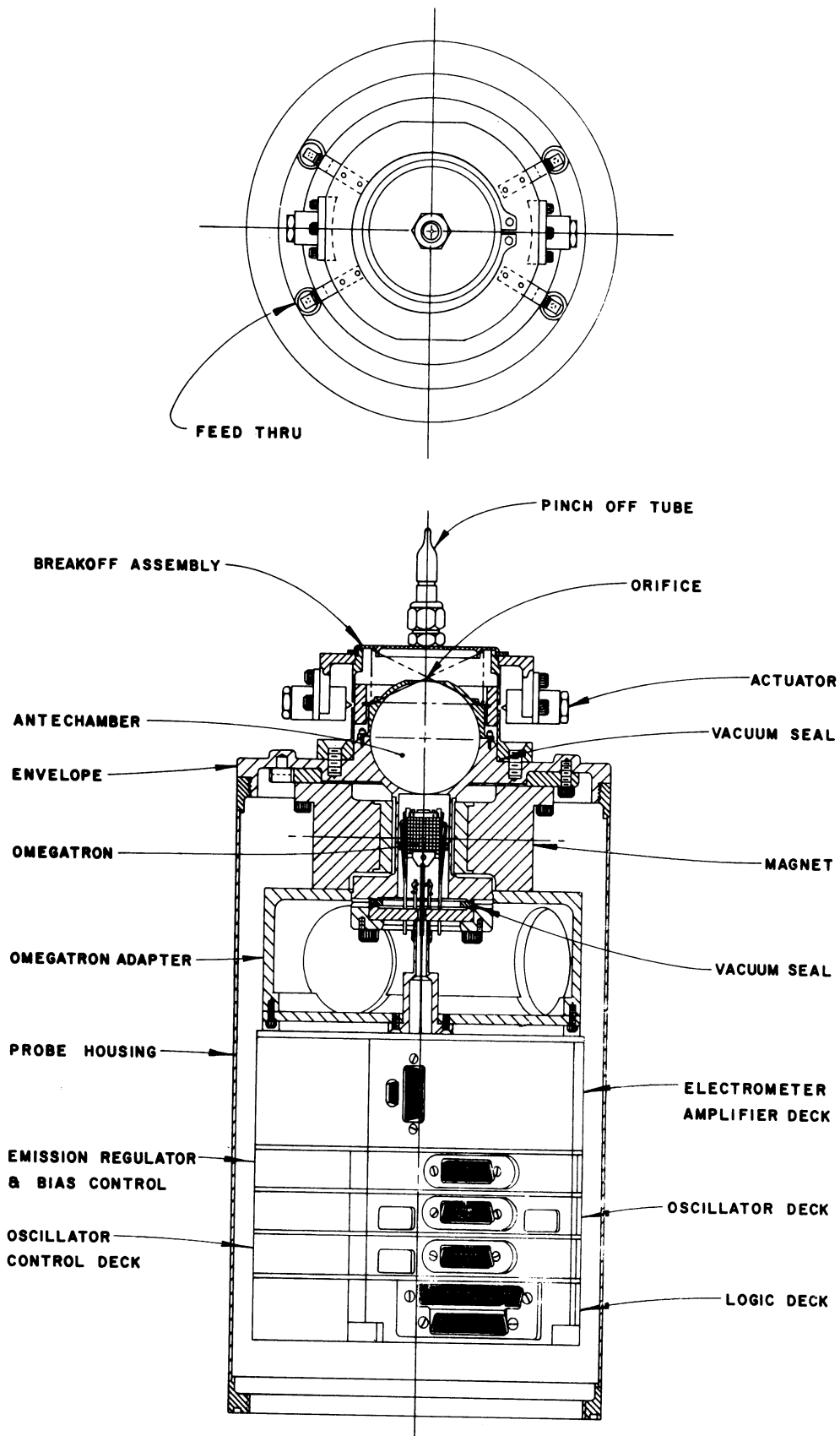


Figure 6. Omegatron II.

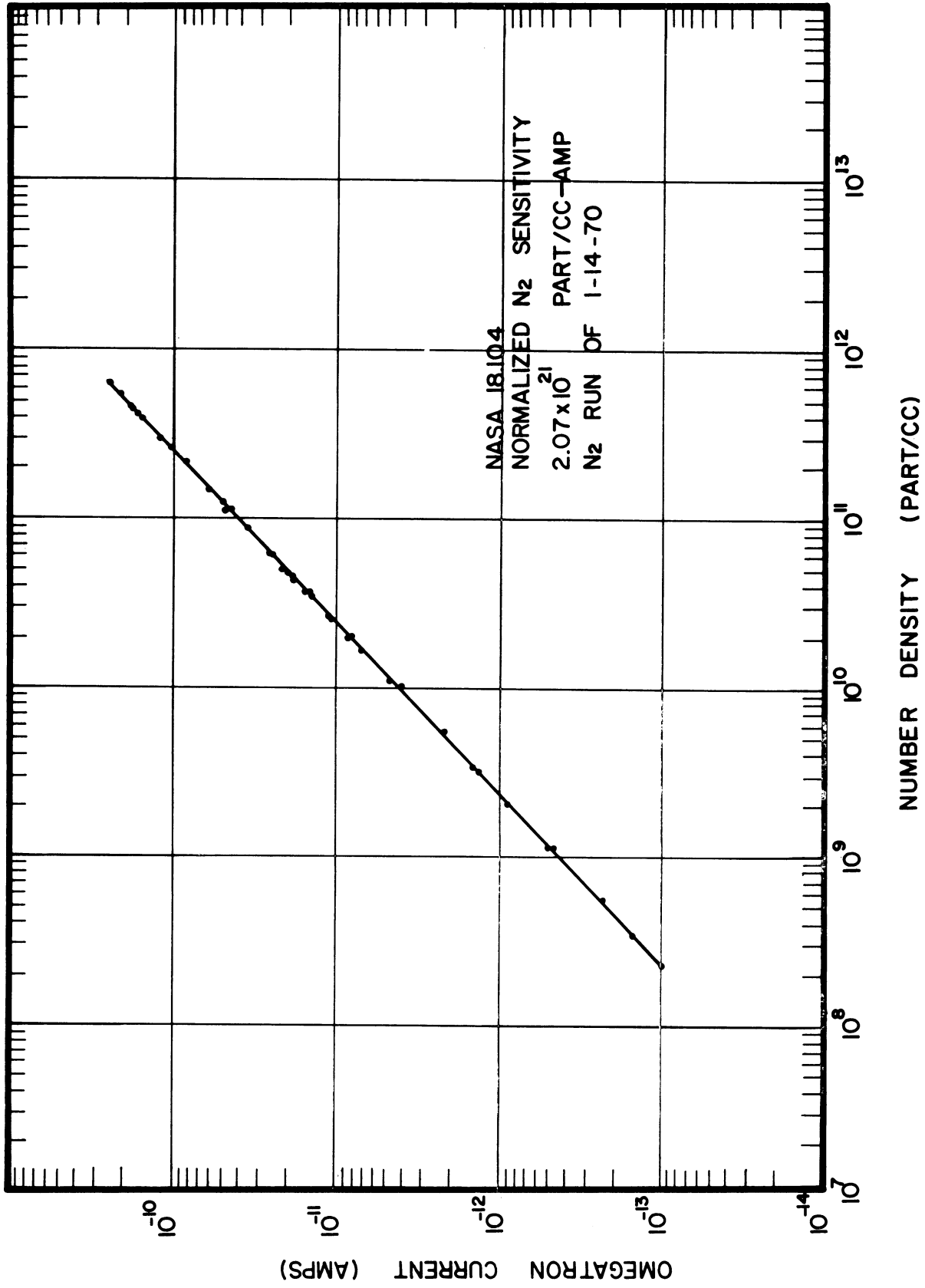


Figure 7. Final calibration of the NASA 18.104 omegatron.

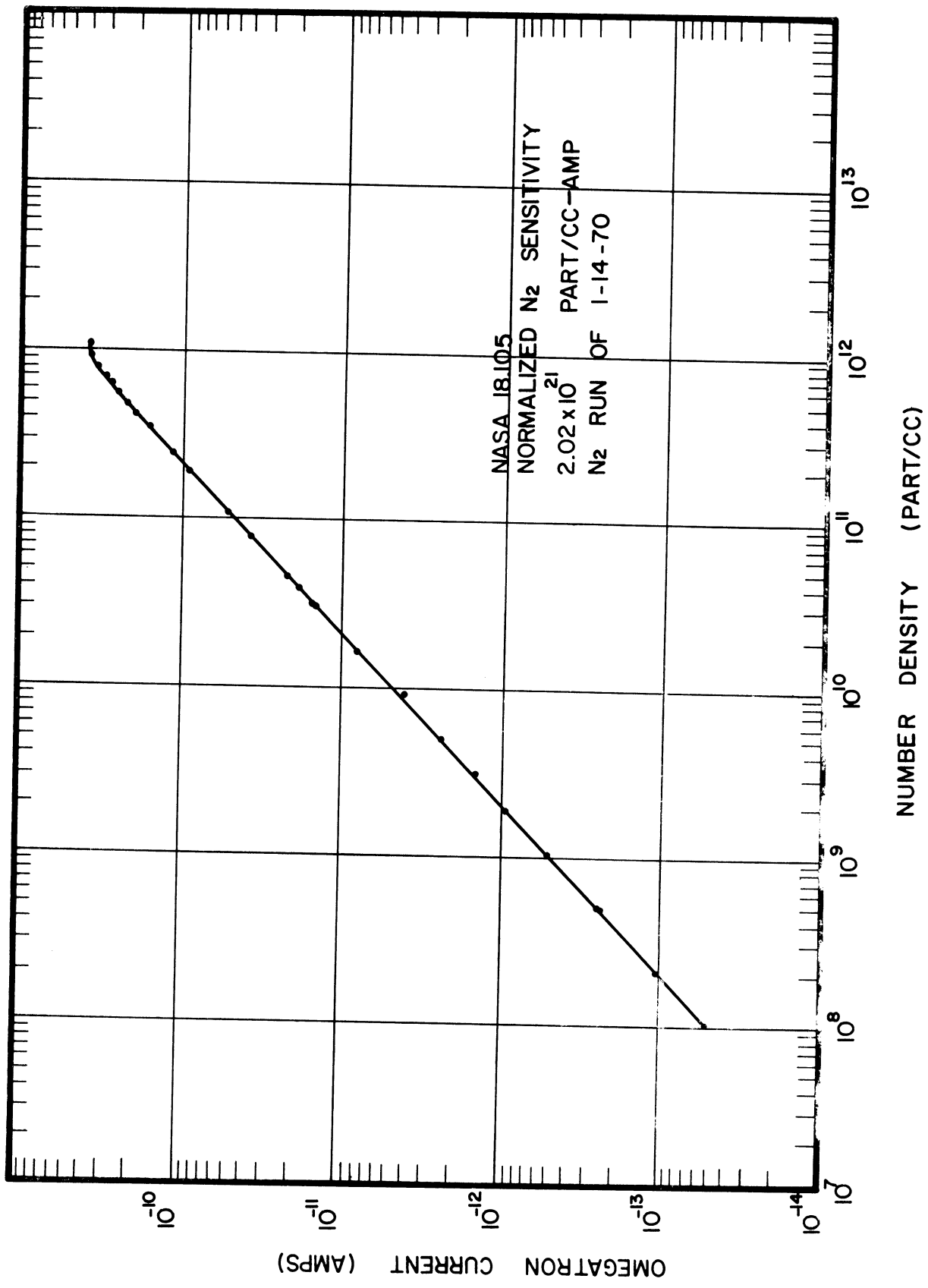


Figure 8. Final calibration of the NASA 18.105 omegatron.

5.2. ELECTRON TEMPERATURE AND DENSITY PROBE

The electron temperature and density probe consists of two cylindrical Langmuir probes placed in the plasma, and an electronics unit which measures the current collected by the probes as they are swept through a series of ramp voltages. A typical Langmuir probe is shown in Figure 9. For both flights probe 1 is stainless steel and probe 2 is rhodium-plated stainless steel.

Each electronics unit consisted of a dc-dc converter, the ΔV ramp generator, a three range current detector, and associated logic and control circuits. Timing and sequencing of the various functions are shown in Figure 10. The pertinent system parameters follow.

	<u>NASA 18.104</u>	<u>NASA 18.105</u>
(a) Input Power	2.2 W at 28 V	2.2 W at 28 V
(b) Sensitivity		
Range 1	4.0 μ A full scale (5 V)	4.0 μ A full scale (5 V)
Range 2	0.4 μ A full scale (5 V)	0.4 μ A full scale (5 V)
Range 3	0.05 μ A full scale (5 V)	0.05 μ A full scale (5 V)
(c) Ramp Voltage (ΔV)		
High ΔV	80.0 V/sec	80.0 V/sec
Low ΔV	24.1 V/sec	24.0 V/sec
Period	124.7 msec	125.1 msec
(d) Output		
Voltage	-0.59 V to +5.65 V	-0.60 V to +6.01 V
Resistance	2700 Ω	2700 Ω
Bias Level	1.01 V	1.02 V
(3) System Calibration		
	Calibration occurs every 31.5 sec for NASA 18.104 and 27.0 sec for NASA 18.105 for a duration of 750 msec.	

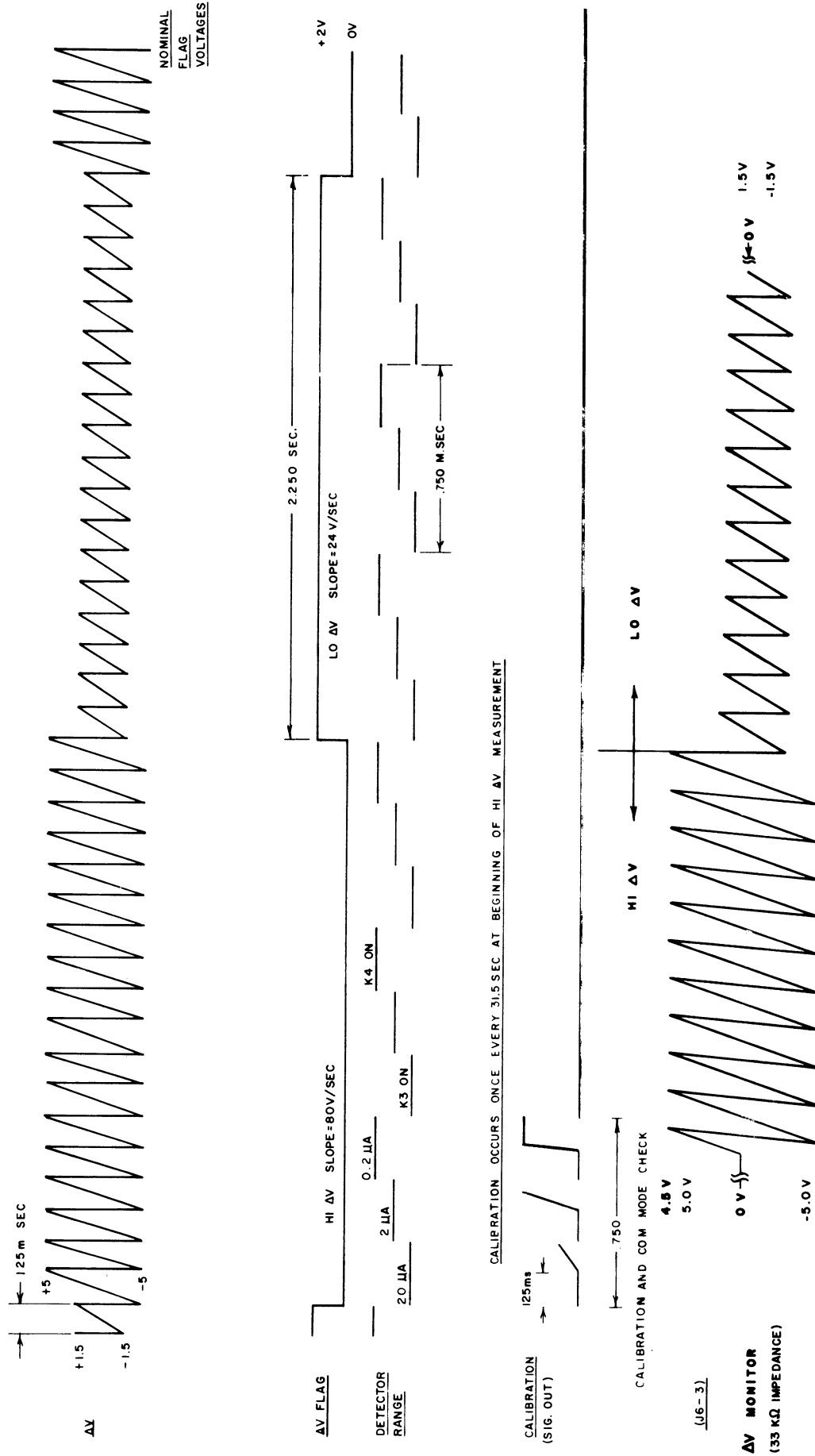


Figure 9. Electron temperature and density probe.

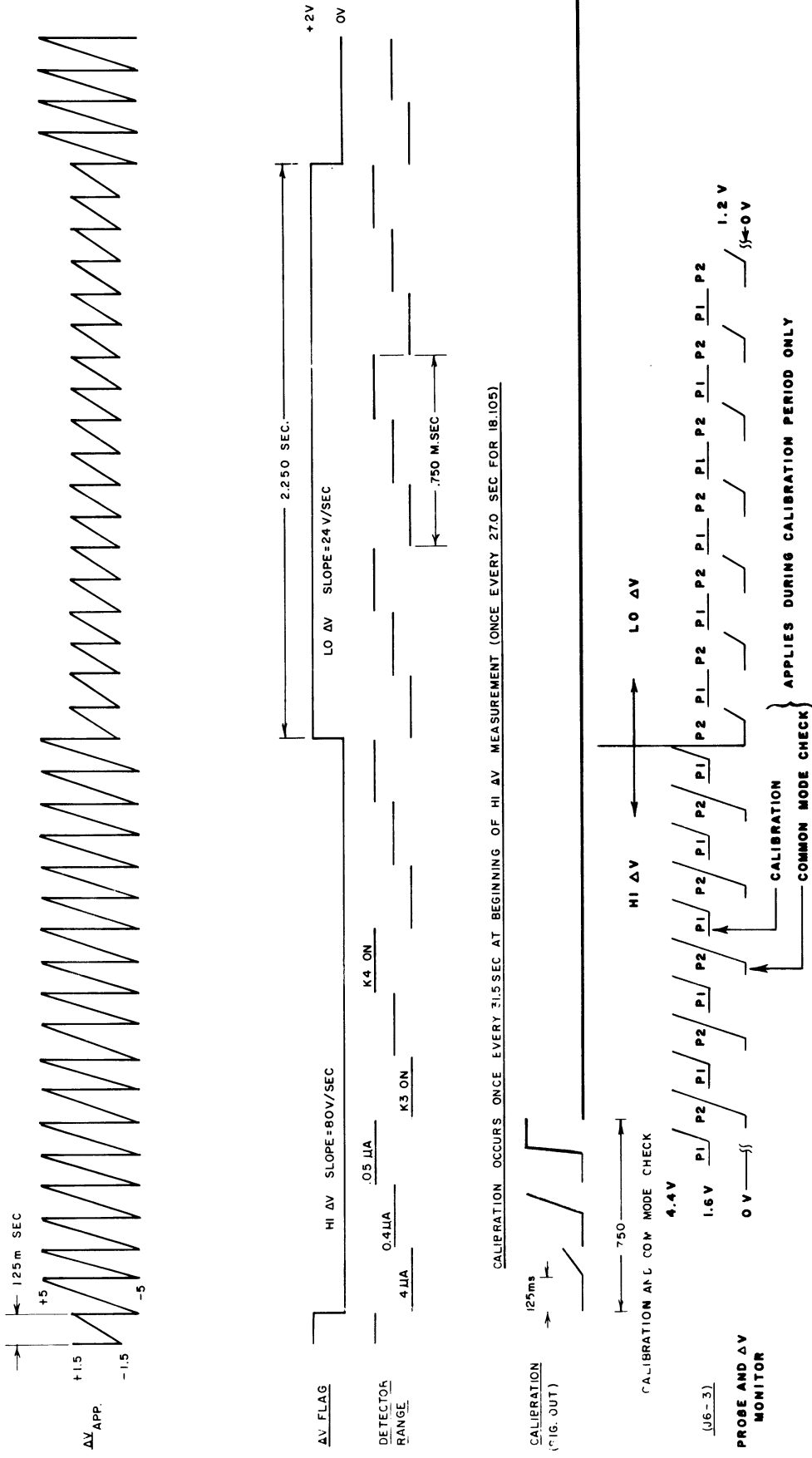


Figure 10. ETD system timing and output format.

5.3.1. Aspect Determination System

The NASA 18.104 and NASA 18.105 TPs used Adcole sensors identical to those used on previous flights. However, each flight used a single-eye (120 deg field of view) system rather than the triple-eye (360 deg field of view) system of previous flights. Also, the accompanying electronics were adjusted at SPRL to account for the solar obscuration encountered.

The 120 deg field of view proved sufficient to determine the NASA 18.104 aspect. The attitude of the TP was determined by using the method of referencing the solar vector and the velocity vector (Carter, 1968). The resulting minimum angle of attack, determined to an estimated accuracy of ± 5 deg, is plotted versus altitude in Figure 11.

Due to an electronics problem the NASA 18.105 sensor failed to function during the flight. However, information obtained from the ion spectrometer (which "saw" the sun) was sufficient to establish the initial parameters necessary for standard reduction of the TP attitude. The resulting minimum angle of attack, determined to an estimated accuracy of ± 5 deg, is plotted versus altitude in Figure 12.

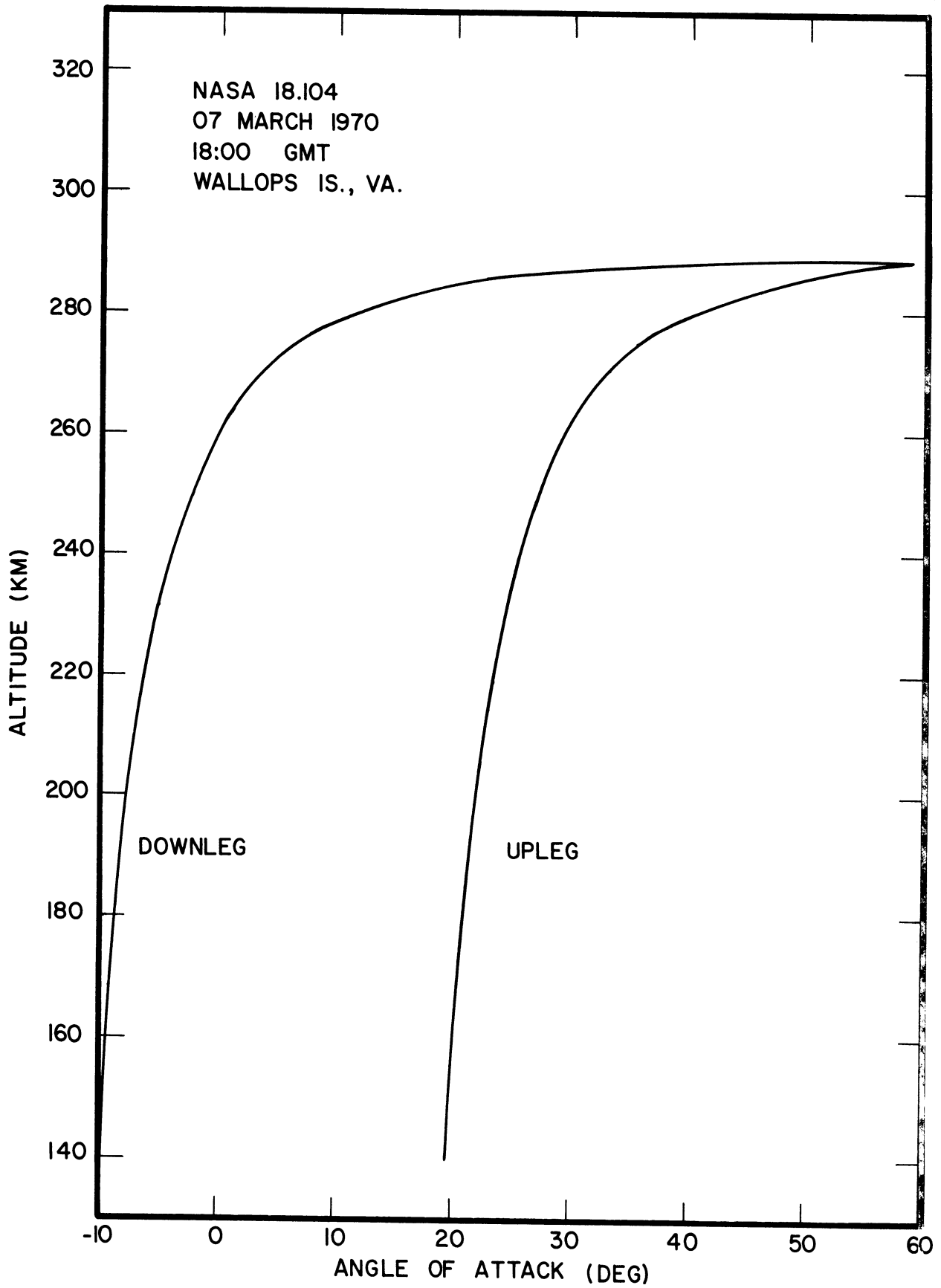


Figure 11. NASA 18.104 minimum angle of attack vs. altitude.

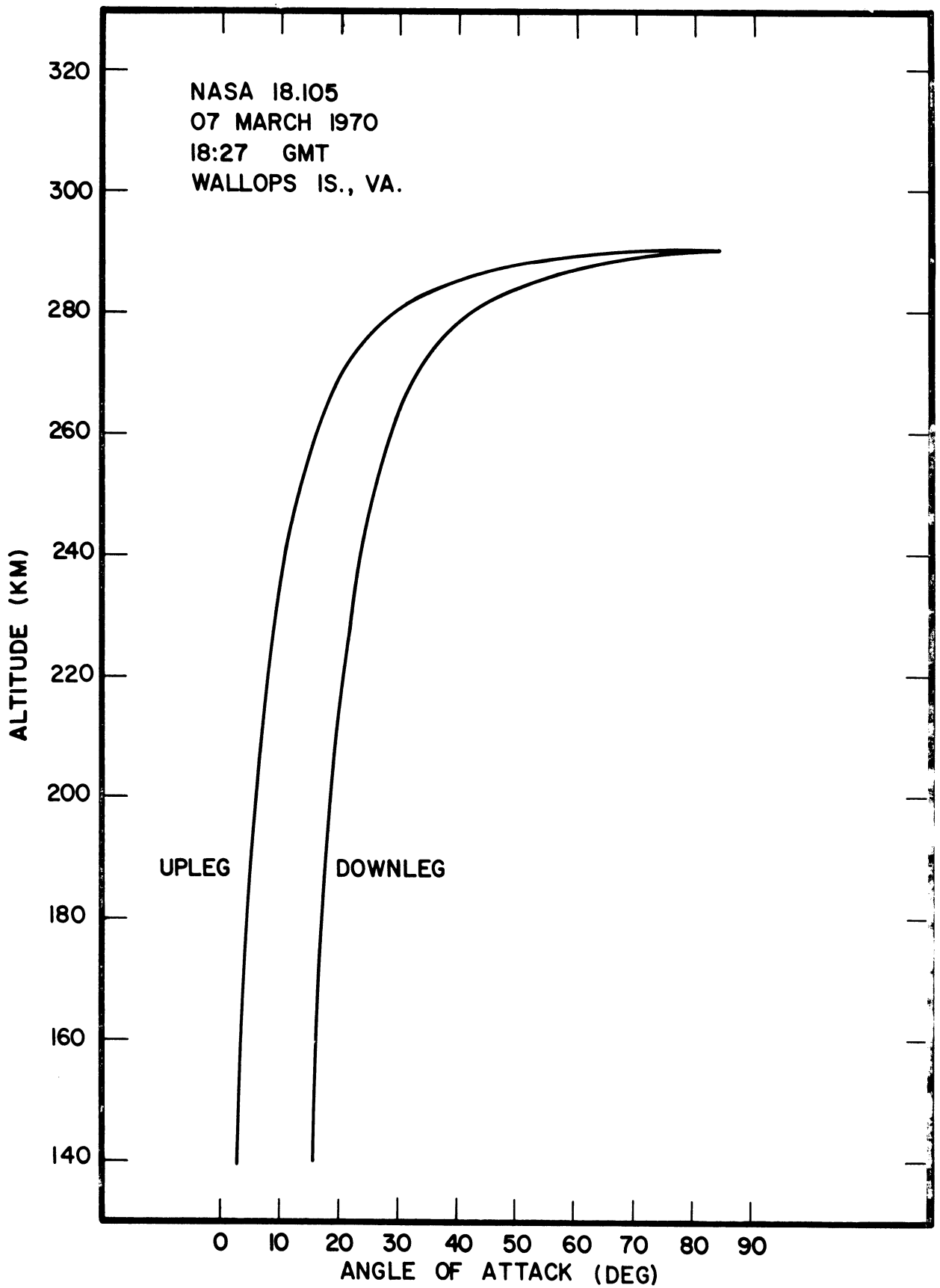


Figure 12. NASA 18.105 minimum angle of attack vs. altitude.

5.3.2. Telemetry

For each flight, the payload data were transmitted in real time by twelve channel PAM/FM/FM telemetry system at 240.2 MHz with a nominal output of 2.5 W. The telemetry system used twelve subcarrier channels, as outlined below.

	<u>NASA 18.104</u>	<u>NASA 18.105</u>
Transmitter:	TRPT-251-1RBO (Serial No. 842)	TRPT-250RA0 (Serial No. 2516)
Power Amplifier:	TRFP-2V (Serial No. 144)	TRFP-2V (Serial No. 450)
Mixer Amplifier:	MMA-12 (Serial No. 11898)	MMA-12 (Serial No. 652)
Subcarrier Channels:	MMO-11	MMO-11

IRIG Band	Serial No.		Center Frequency	Function	Low Pass Filter Used
	18.104	18.105			
20	8356	7510	124 kHz	IS Digital	2500 Hz CA
18	16666	16673	70 kHz	OM OUT/S	450 Hz CA
17	19232	20386	52.5 kHz	ESP/D	790 Hz CD
16	7831	404	40 kHz	IS Analog 1	600 Hz CA
15	606	15015	30 kHz	IS Analog 2	450 Hz CA
14	15163	9052	22 kHz	IS Analog 3	330 Hz CA
13	15270	15278	14.5 kHz	IS Ramp	220 Hz CA
12	18742	12583	10.5 kHz	Aspect	330 Hz CA
11	15902	15997	7.35kHz	Commutator	120 Hz CD
10	7808	15428	5.4 kHz	OM OUT/D	80 Hz CD
9	15777	15728	3.9 kHz	OM Range	60 Hz CD
8	674	15667	3.0 kHz	IS V _s Monitor	45 Hz CD

Instrumentation power requirements for each flight totaled approximately 35 W, supplied by a Yardney HR-1 Silvercell battery pack of a nominal 28 V output.

5.3.3. Housekeeping Monitors

Outputs from various monitors throughout the instrumentation provided information bearing on the operations of the electronic components during the flights. These outputs were fed to a thirty-segment commutator which ran at one rps. The commutator assignments were as follows:

COMMUTATOR FORMAT FOR NASA 18.104 AND NASA 18.105

Segment Number	Segment Assignment
1	OUT/D
2	OUT/S Range
3	RF Frequency
4	RF Amplitude
5	Automatic Frequency Control Lock
6	DC Frequency Control
7	Beam Current
8	Filament Voltage
9	Internal Pressure Monitor
10	Thermistor - Gauge Temperature
11	Thermistor - Amplifier Temperature
12	Thermistor - Transmitter Temperature
13	Battery Voltage Monitor
14	+15 Power Supply Voltage
15	RF Voltage Monitor
16	G15 Monitor
17	Sweep Voltage Monitor
18	Thermistor 1
19	Thermistor 2
20	+10 Power Supply Voltage
21	RF Voltage Monitor
22	+3 Power Supply Voltage
23	Sweep Voltage Monitor
24	0 V Calibration
25	1 V Calibration
26	2 V Calibration
27	3 V Calibration
28	4 V Calibration
29	5 V Calibration
30	5 V Calibration

6. ANALYSIS OF DATA

The telemetered data were recorded on magnetic tape at the Wallops Island Main Base and the GSFC Station A ground station facilities. Appropriate paper records were made from the magnetic masters, facilitating "quick look" evaluations. The aspect data were reduced to engineering parameters from paper records. The omegatron and housekeeping data were reduced by computer techniques from the magnetic tapes.

6.1. TRAJECTORY AND ASPECT

The position and velocity data used to determine aspect, ambient N_2 density, and ambient temperature as a function of time and altitude were obtained by fitting a smooth theoretical trajectory to the FPQ-6 radar data. The theoretical trajectory is programmed for computer solution similar to that described by Parker (1962). The analysis of minimum angle of attack (α_{\min}) as described by Carter (1968) is also incorporated in the program. The output of the computer furnishes α_{\min} , altitude, and velocity as a function of time. Plots of α_{\min} versus altitude have already been given in Figures 11 and 12. Figures 13 and 14 show the occurrence of significant events during the flights.

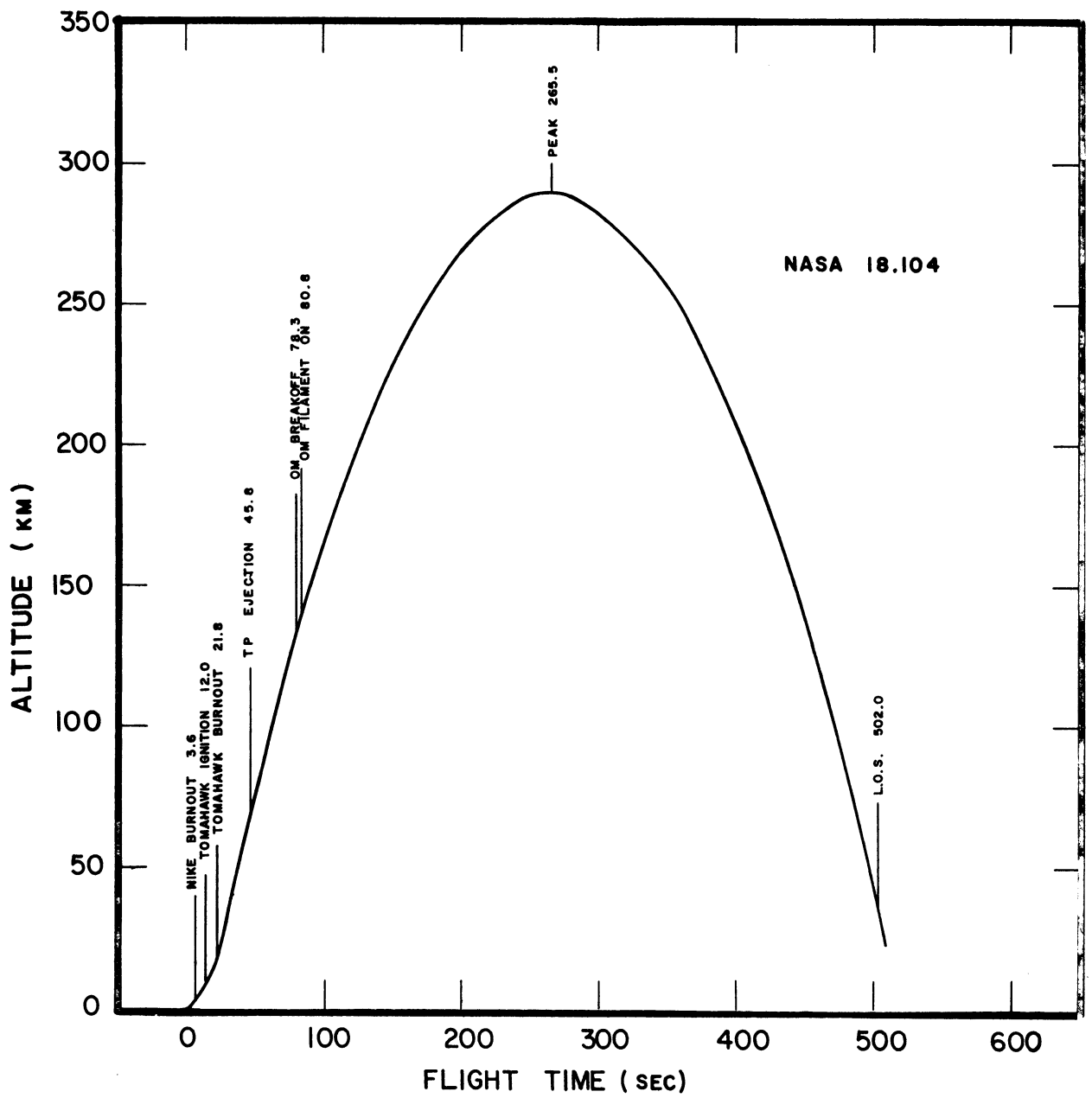


Figure 13. NASA 18.104 sequence of events.

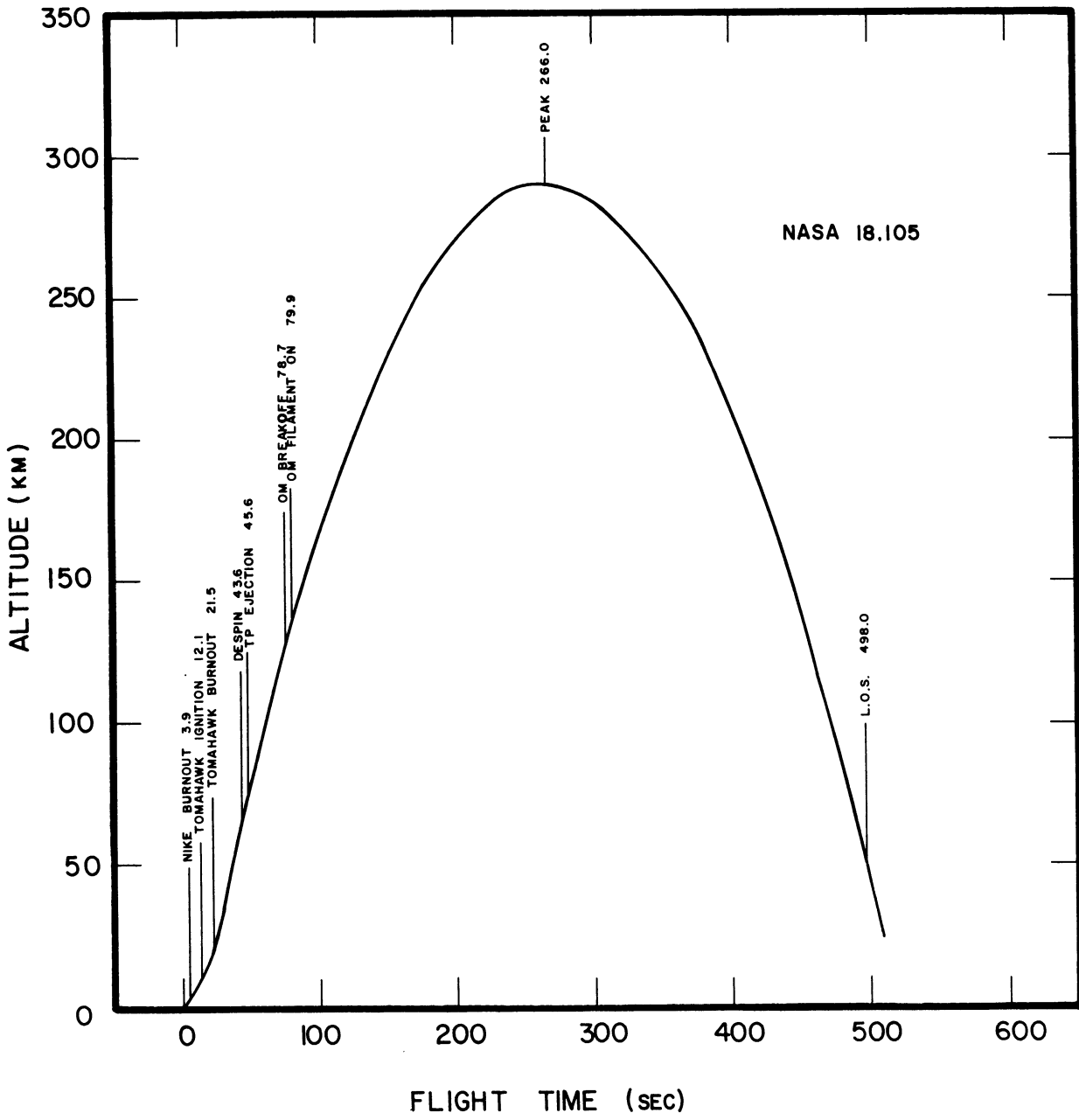


Figure 14. NASA 18.105 sequence of events.

6.2. AMBIENT N₂ DENSITY

The neutral molecular nitrogen density was determined from the measured gauge partial pressure as described by Spencer, et al. (1965, 1966), using the basic relationship:

$$n_a = \left(\frac{\Delta n_i u_i}{2 \sqrt{\pi} V \cos \alpha_{\min}} \right) K(S_o, \alpha)$$

where

n_a = ambient N₂ number density

Δn_i = maximum minus minimum gauge number density during one tumble, $A \times \Delta I$, where A is the sensitivity of the gauge

u_i = $\sqrt{2KT_i/m}$, most probable thermal speed of particles inside gauge

T_i = gauge wall temperature

V = vehicle velocity with respect to the earth

α_{\min} = minimum angle of attack for one tumble

$K(S_o, \alpha)$ = the reciprocal of the normalized transmission probability as defined by Ballance (1967), referred to as the geometry correction factor.

ΔI , the difference between the maximum (peak) omegatron gauge current and the minimum (background) gauge current versus flight time is shown in Figures 15 and 16. The background current is the result of the outgassing of the gauge walls, and the inside density is due to atmospheric particles which have enough translational energy to overtake the payload and enter the gauge. The outgassing component is assumed constant for one tumble and affects both the peak reading and the background reading, and, therefore, does not affect the difference. From calibration data obtained by standard techniques, the inside number density, Δn_i , is computed for the measured current.

By using the measured gauge wall temperature, the most probable thermal speed of the particles inside the gauge, u_i , is computed. The uncertainty in this measurement is believed to be about $\pm 2\%$ absolute.

V , the vehicle velocity with respect to the earth is obtained from the

trajectory curve fitting described previously and is believed to be better than $\pm 1\%$ absolute.

$\cos \alpha_{\min}$ is obtained from the aspect analysis described by Carter (1968). Since the uncertainty in $\cos \alpha_{\min}$ depends upon α_{\min} , for any given uncertainty in α_{\min} , each particular case and altitude range must be considered separately. Figures 11 and 12 show that the minimum angle of attack for the upleg is generally less than 20 degrees, so with an assumed maximum uncertainty in α_{\min} of ± 5 degrees, the resulting uncertainty in $\cos \alpha_{\min}$ is less than $\pm 3\%$. The data for low angle of attack were used as control data.

$K(S_0, \alpha)$, the geometry correction factor versus altitude, is shown in Figures 17 and 18. As can be seen, the maximum correction is about 6%, or $K(S_0, \alpha) = .94$ at about 140 km altitude for the upleg data. The correction factor, determined from empirical and theoretical studies, is believed known to better than 2%.

The resulting ambient N_2 number density, obtained from the measured quantities described above, is shown in Figures 19 and 20 and is tabulated in Table III. The uncertainty in the ambient density due to the combined uncertainties in the measured quantities is thought to be 10% relative and 25% absolute.

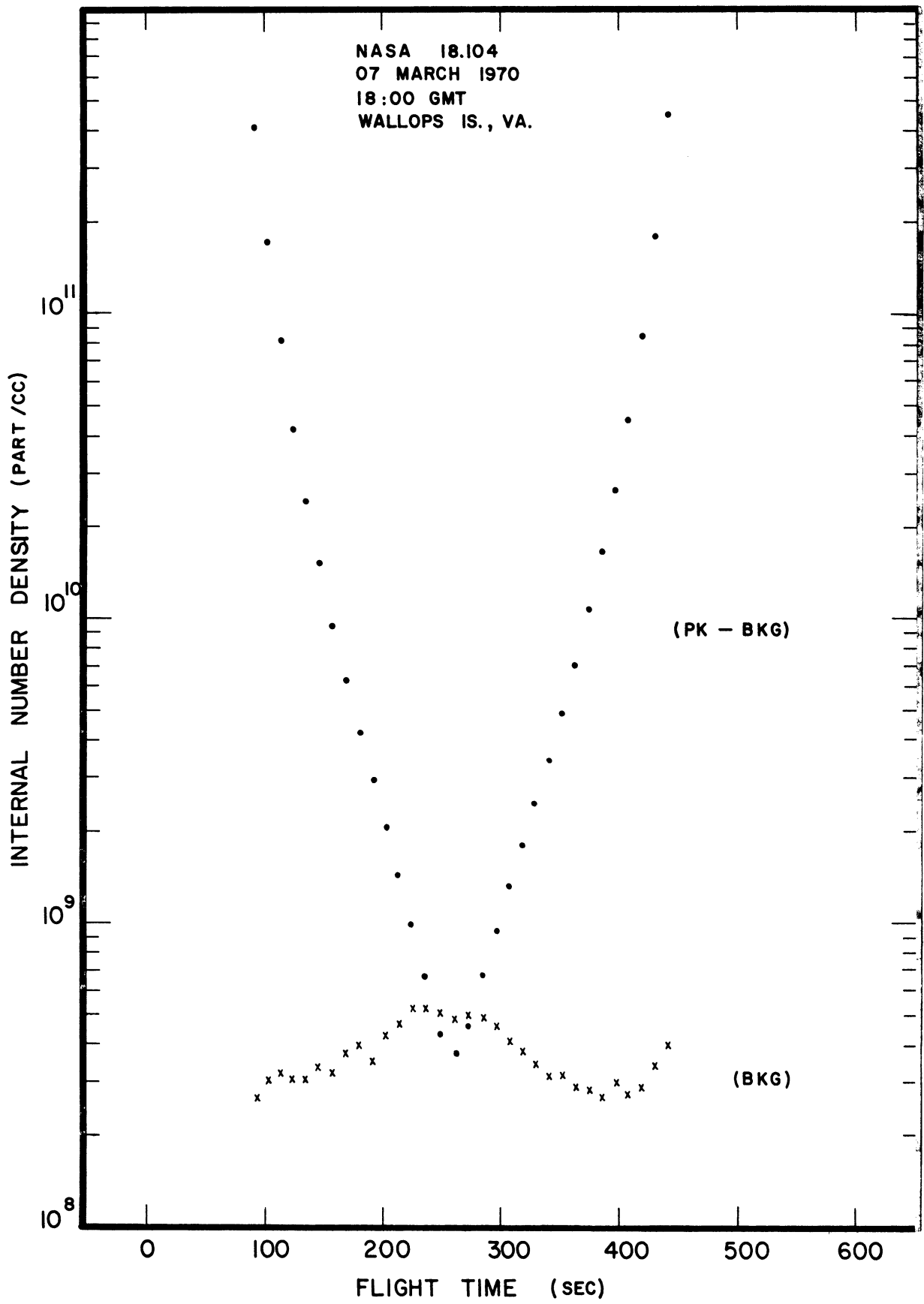


Figure 15. NASA 18.104 omegatron current vs. flight time.

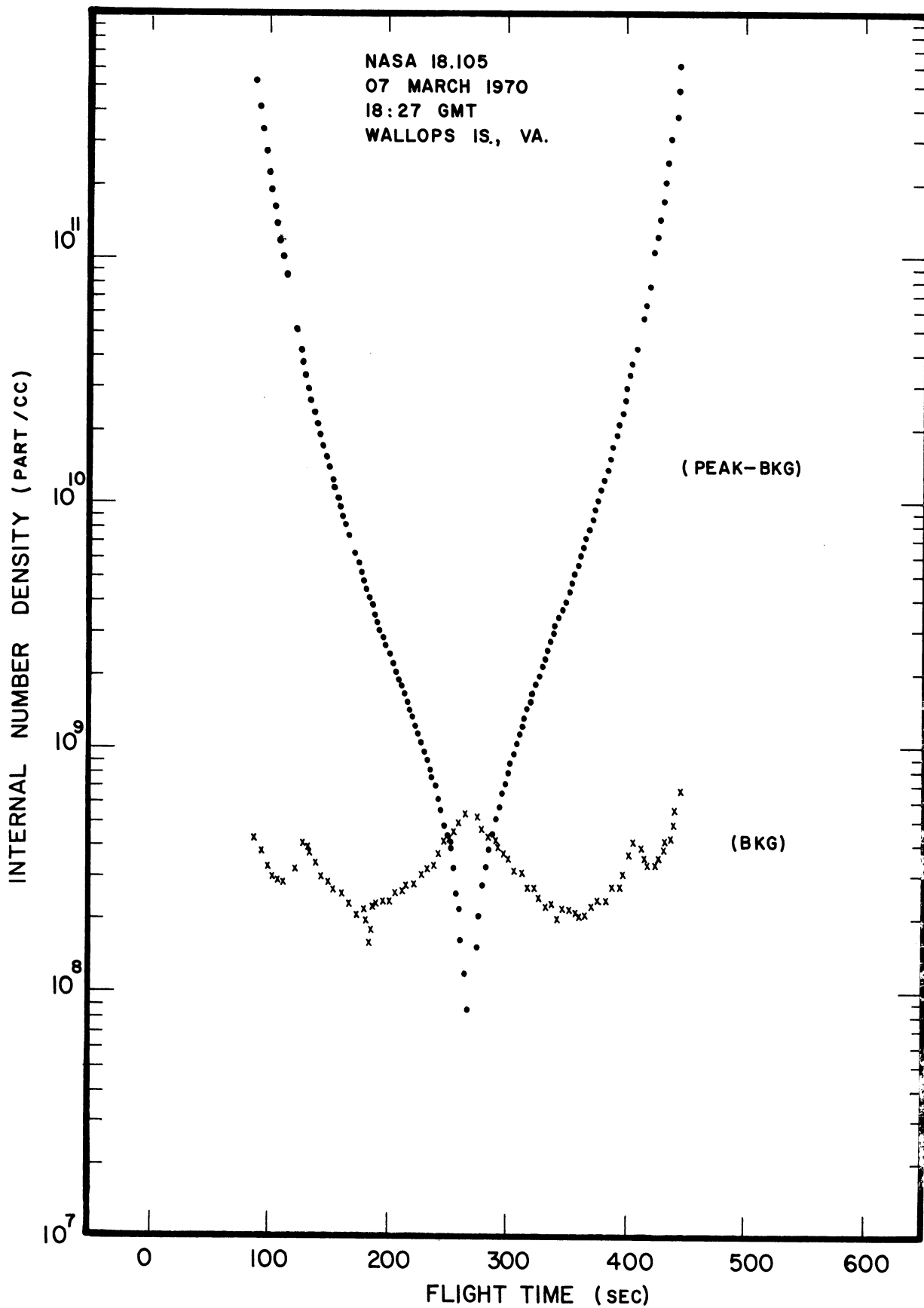


Figure 16. NASA 18.105 omegatron current vs. flight time.

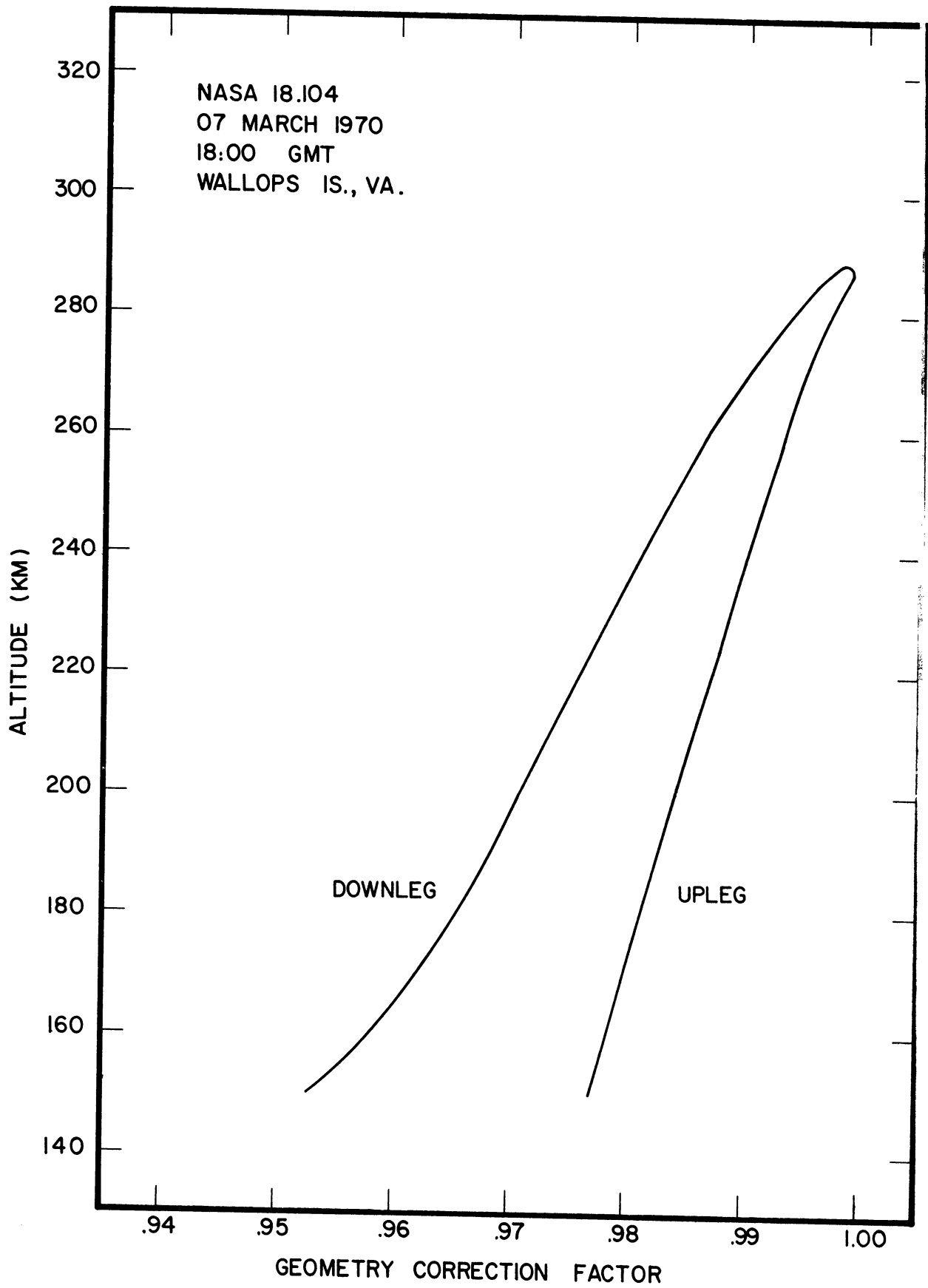


Figure 17. $K(S_o, \alpha)$ vs. altitude for NASA 18.104.

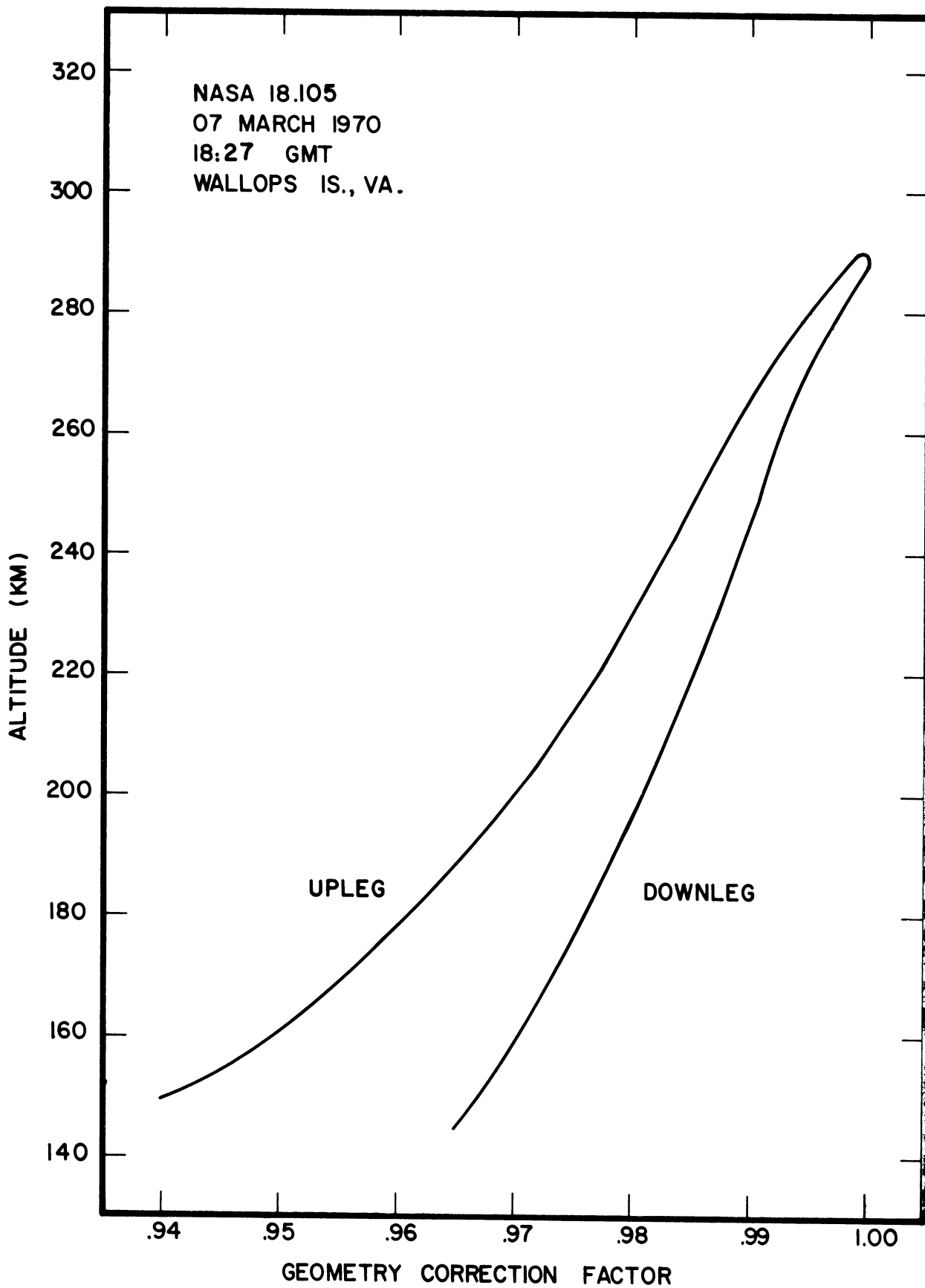
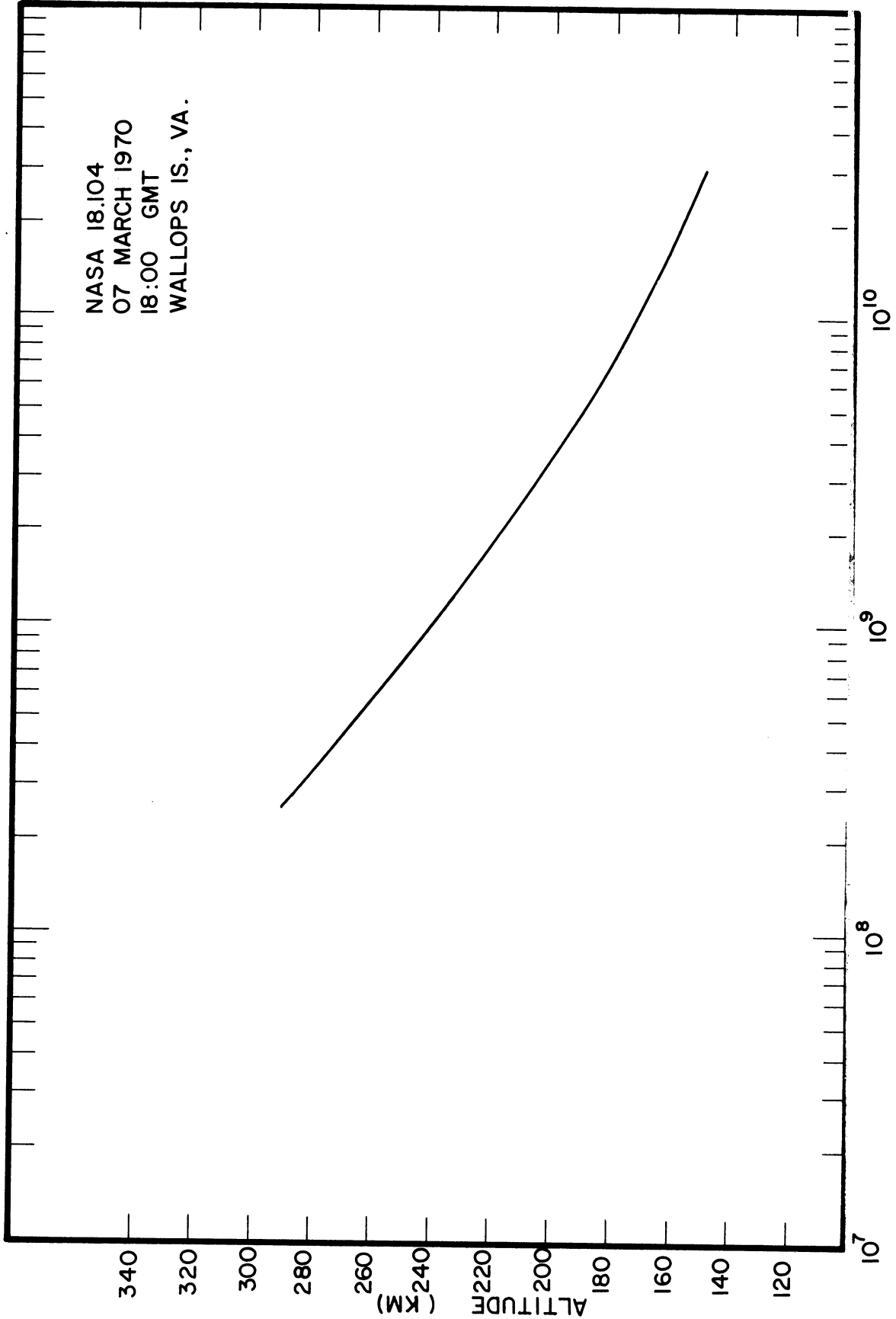
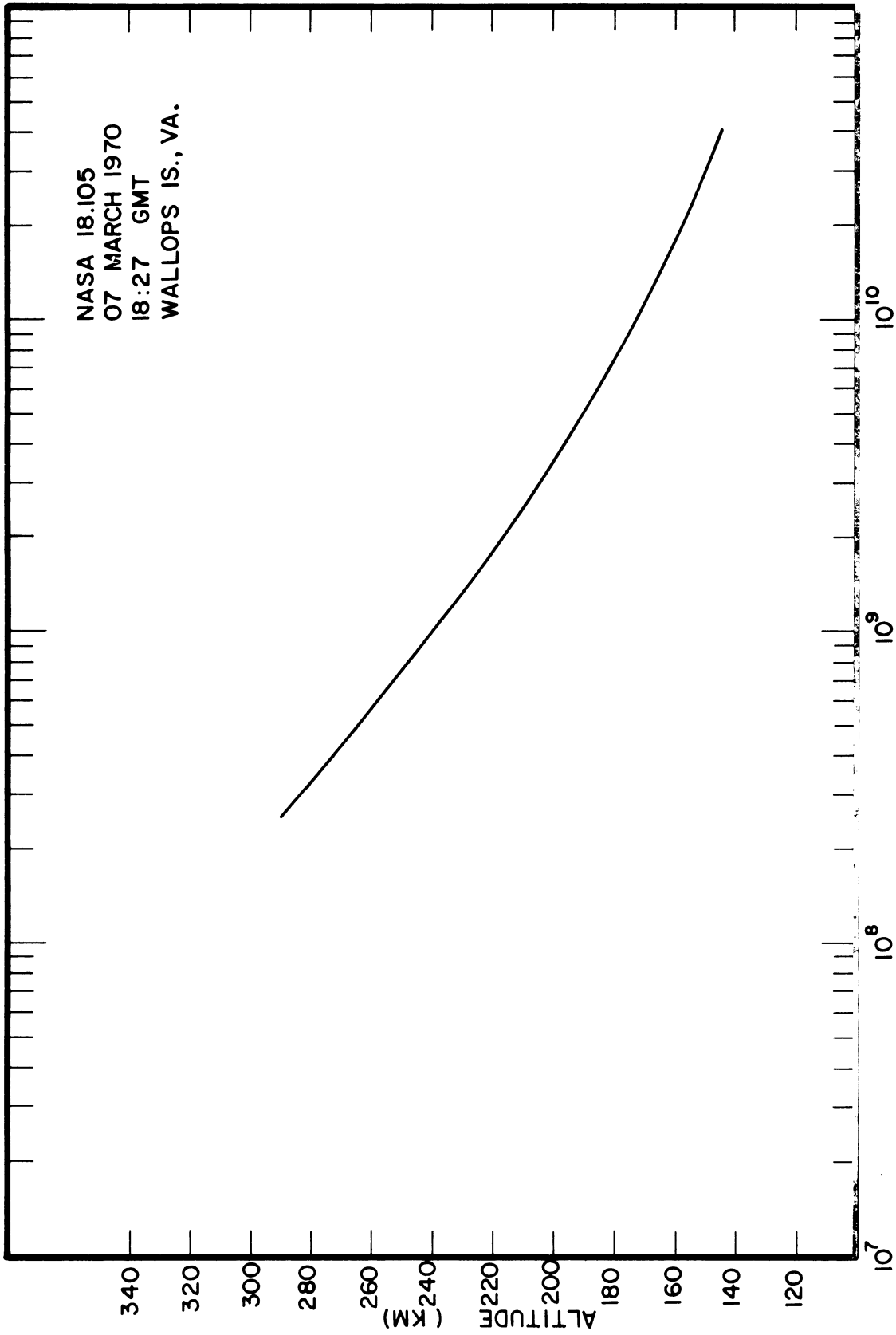


Figure 18. $K(S_0, \alpha)$ vs. altitude for NASA 18.105.



AMBIENT N₂ DENSITY (PART/CC)

Figure 19. NASA 18.104 ambient N₂ density vs. altitude.



AMBIENT N₂ DENSITY (PART/CC)

Figure 20. NASA 18.105 ambient N₂ density vs. altitude.

TABLE III

 N_2 AMBIENT DENSITY DATA

NASA 18.104

7 March 1970

18:00 GMT

13:00 EST

Wallops Island, Virginia

Altitude (km)	Temperature (°K)	Density (part/cc)
150	712	3.05×10^{10}
155	749	2.34
160	785	1.82
165	820	1.43
170	853	1.14×10^{10}
175	885	9.17×10^9
180	918	7.44
185	945	6.11
190	971	5.05
195	993	4.21
200	1013	3.54
205	1029	2.99
210	1044	2.53
215	1056	2.16
220	1068	1.85
225	1078	1.59
230	1087	1.36
235	1095	1.18
240	1103	1.02×10^9
245	1110	8.80×10^8
250	1116	7.63
255	1122	6.62
260	1128	5.75
265	1133	5.00
270	1138	4.36
275	1143	3.80
280	1148	3.31
285	1154	2.89
289	1157	2.60×10^8

Fit Parameters: $T_\infty = 1185 \text{ }^\circ\text{K}$
 $T_0 = 701 \text{ }^\circ\text{K at } 150 \text{ km}$
 $P_b = 3.03 \times 10^{-8} \text{ torr}$
 $\sigma = 2.00 \times 10^{-2}$

TABLE III (Concluded)

NASA 18.105
 7 March 1970
 18:27 GMT
 13:27 EST
 Wallops Island, Virginia

Altitude (km)	Temperature (°K)	Density (part/cc)
145	676	4.08×10^{10}
150	712	3.09
155	746	2.37
160	781	1.84
165	814	1.45
170	846	1.16×10^{10}
175	881	9.30×10^9
180	914	7.54
185	944	6.16
190	972	5.07
195	996	4.21
200	1018	3.53
205	1036	2.98
210	1052	2.53
215	1066	2.15
220	1078	1.84
225	1088	1.58
230	1097	1.37
235	1105	1.18
240	1113	1.02×10^9
245	1119	8.86×10^8
250	1125	7.70
255	1130	6.69
260	1135	5.83
265	1139	5.08
270	1143	4.43
275	1146	3.86
280	1149	3.38
285	1151	2.95
290	1153	2.58×10^8

Fit Parameters: $T_\infty = 1168 \text{ }^\circ\text{K}$
 $T_0 = 837 \text{ }^\circ\text{K}$ at 170 km
 $P_b = 3.09 \times 10^{-8}$ torr
 $\sigma = 2.60 \times 10^{-2}$

6.3. TEMPERATURE

The ambient temperatures shown in Figures 21 and 22 and tabulated in Table III were obtained by integrating the hydrostatic equation using the measured N_2 density profile to obtain a partial pressure profile, and by relating the known density and pressure to the temperature through the ideal gas law. In this procedure the assumptions of hydrostatic equilibrium and perfect gas behavior are implicit. It can be shown that the density integral is stable and highly convergent when carried out in the direction of increasing density. The pressure or temperature at the initial (upper) boundary of integration is determined analytically by means of a least squares fitting procedure using a fitting function based on the empirical expression for the temperature profile given by Jacchia (1964), and more particularly by Walker (1965). The procedure is described in detail by Simmons (1969). The fit parameters listed in Table III are the apparent exospheric temperature (T_∞), the reference temperature at the lower boundary (T_0), the apparent N_2 partial pressure at the upper boundary (P_b), and an estimate of the exponential model shape factor (σ).

6.4. GEOPHYSICAL INDICES

The 10.7 cm solar flux ($F_{10.7}$) and the geomagnetic activity indices (a_p) for the appropriate periods are shown in Figures 23 and 24.

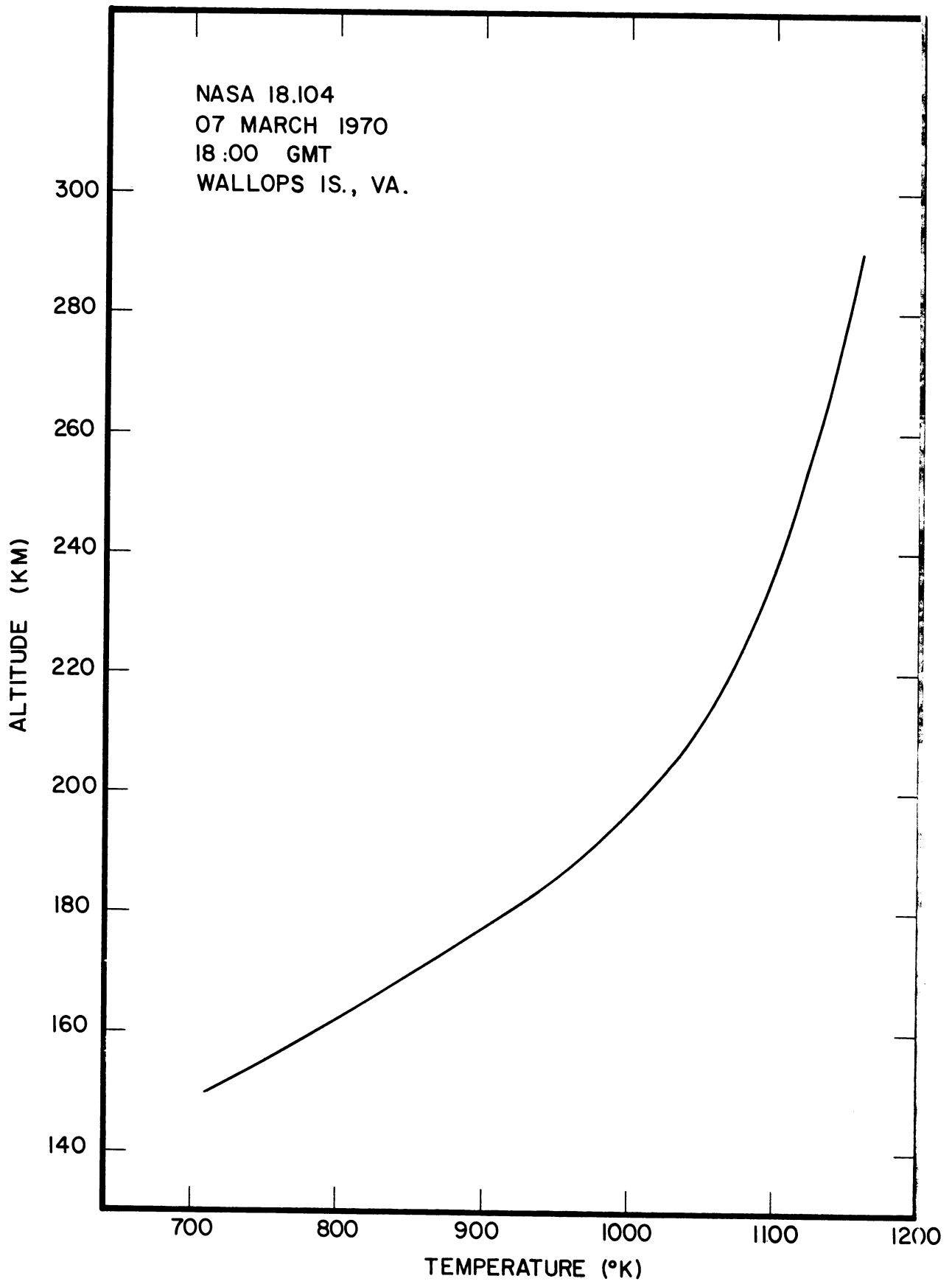


Figure 21. NASA 18.104 neutral particle temperature vs. altitude.

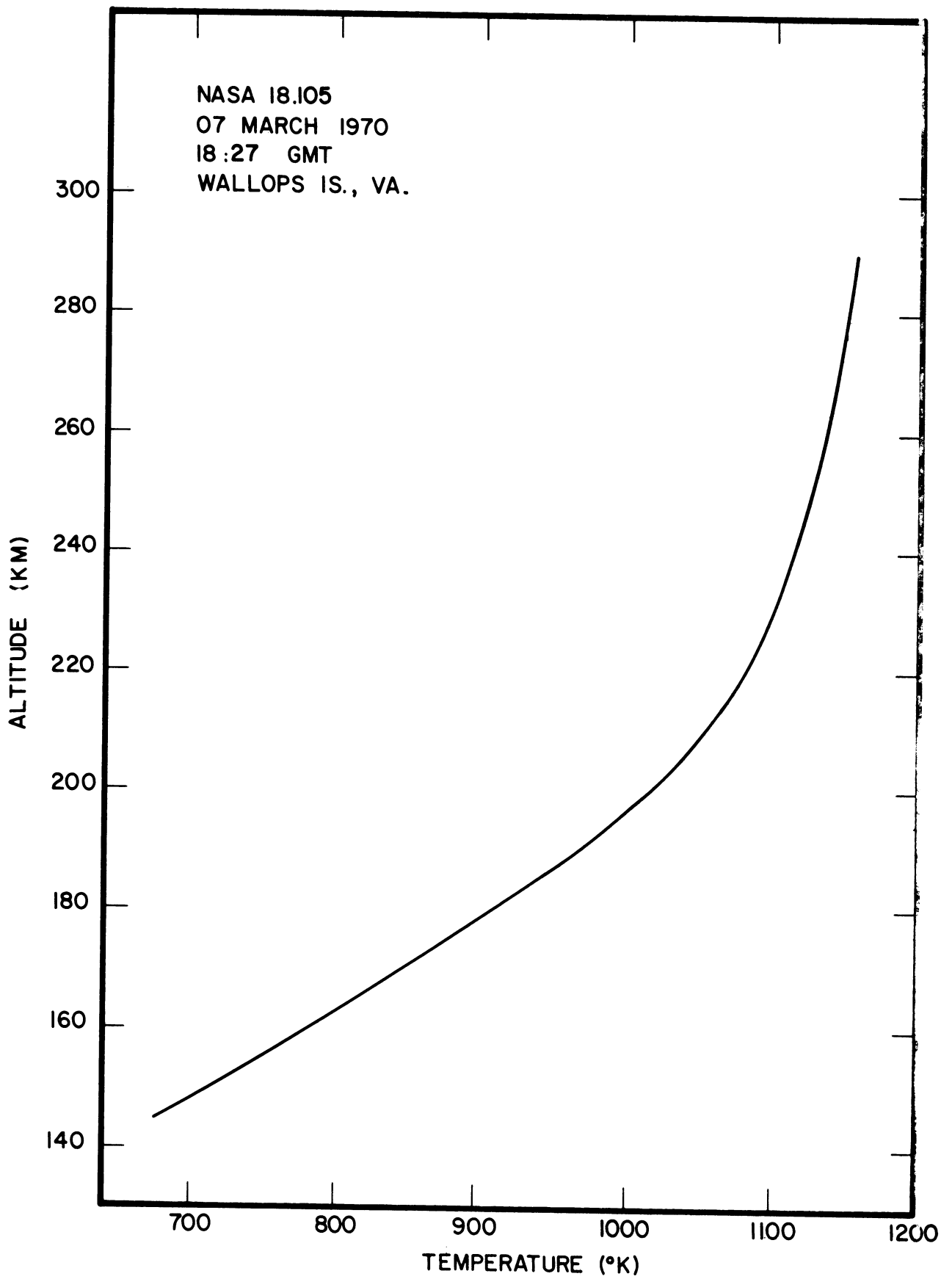


Figure 22. NASA 18.105 neutral particle temperature vs. altitude.

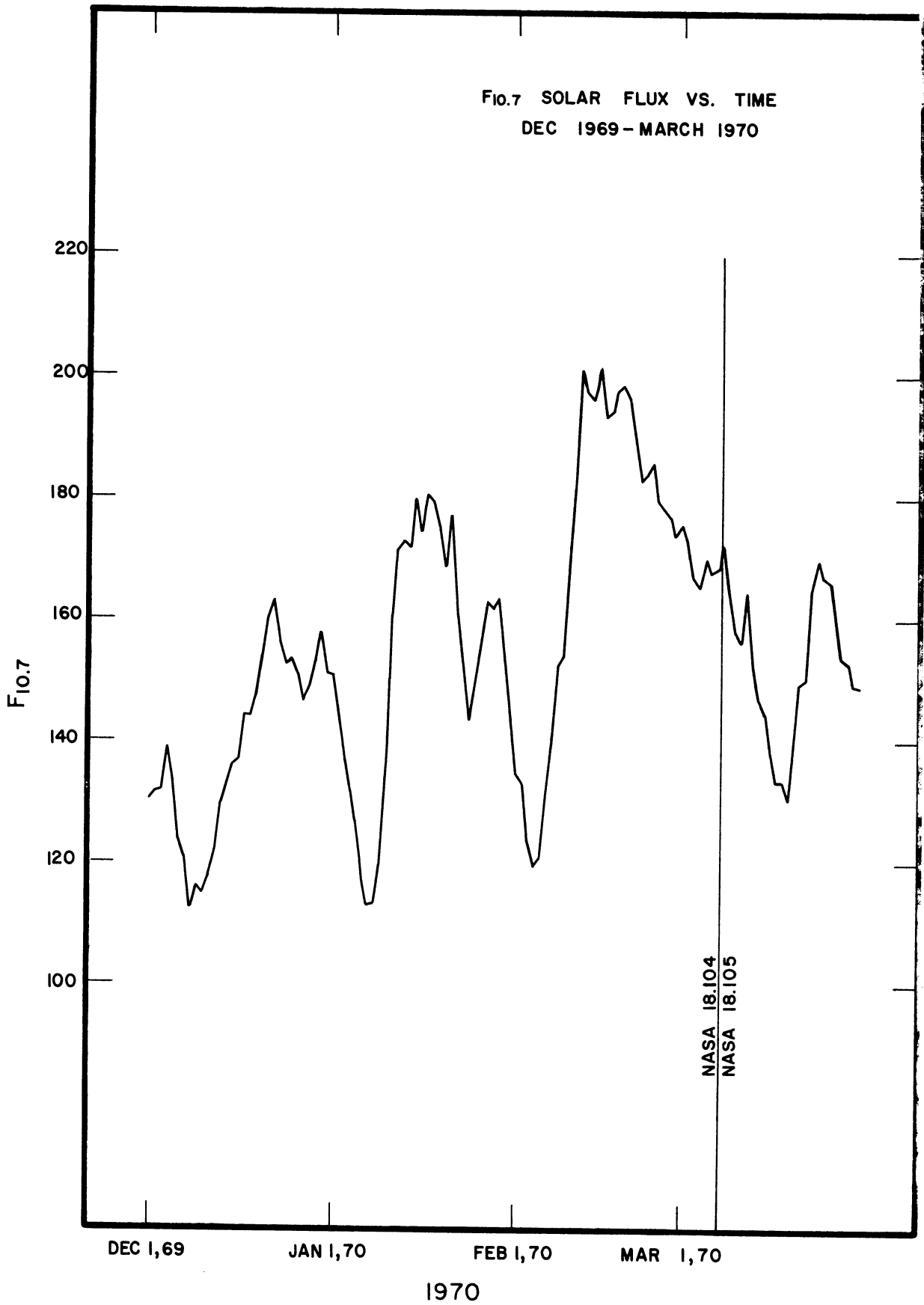


Figure 23. Solar flux at 10.7 cm wavelength.

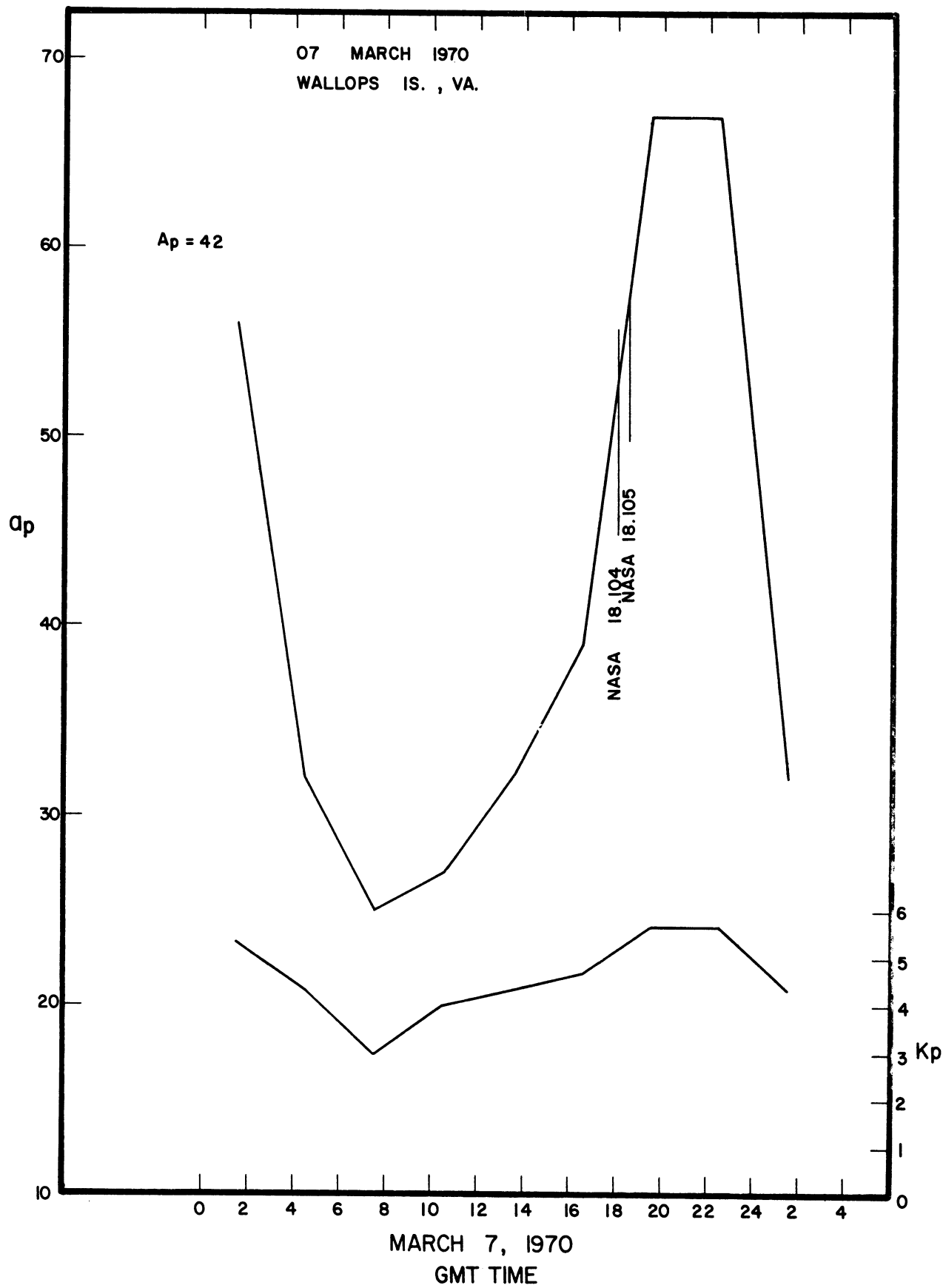


Figure 24. Three-hour geomagnetic activity index (a_p).

7. REFERENCES

- Ballance, James O., An Analysis of the Molecular Kinetics of the Thermosphere Probe, George C. Marshall Space Flight Center, NASA Technical Memorandum, NASA TM X-53641, July 31, 1967.
- Carter, M. F., The Attitude of the Thermosphere Probe, University of Michigan Scientific Report 07065-4-S, April 1968.
- Jacchia, L. G., Static Diffusion Models of the Upper Atmosphere with Empirical Temperature Profiles, Research in Space Science, Smithsonian Astrophysical Observatory Special Report No. 170, 1964.
- Niemann, H. B., and Kennedy, B. C., "An Omegatron Mass Spectrometer for Partial Pressure Measurements in Upper Atmosphere," Review of Scientific Instruments, 37, No. 6, 722, 1966.
- Parker, L. T., Jr., A Mass Point Trajectory Program for the DCD 1604 Computer, Technical Document Report AFSW-TDR-49, Air Force Special Weapons Center, Kirtland Air Force Base, New Mexico, August, 1962.
- Simmons, R. W., NASA 18.49 Thermosphere Probe Experiment, University of Michigan Sounding Rocket Flight Report 07065-9-R, May 1969.
- Spencer, N. W., Brace, L. H., and Carignan, G. R., "Electron Temperature Evidence for Nonthermal Equilibrium in the Ionosphere," Journal of Geophysical Research, 67, 151-175, 1962.
- Spencer, N. W., Brace, L. H., Carignan, G. R., Taeusch, D. R., and Niemann, H. B., "Electron and Molecular Nitrogen Temperature and Density in the Thermosphere," Journal of Geophysical Research, 70, 2665-2698, 1965.
- Spencer, N. W., Taeusch, D. R., and Carignan, G. R., N₂ Temperature and Density Data for the 150 to 300 Km Region and Their Implications, Goddard Space Flight Center, NASA Technical Note X-620-66-5, December 1965.
- Taeusch, D. R., Carignan, G. R., Niemann, H. B., and Nagy, A. F., The Thermosphere Probe Experiment, University of Michigan Rocket Report 07065-1-S, March 1965.
- Walker, J.C.G., "Analytic Representation of Upper Atmosphere Densities Based on Jacchia's Static Diffusion Models," Journal of Atmospheric Sciences, 22, No. 4, 462-463, July 1965.

UNIVERSITY OF MICHIGAN



3 9015 03026 7515